THESIS FOR THE DEGREE OF DOCTOR OF PHILOSOPHY

Fluidized-Bed Reactor Systems for Chemical-Looping Combustion with Inherent Separation of CO_2

EVA JOHANSSON

Department of Energy and Environment
Division of Energy Technology
CHALMERS UNIVERSITY OF TECHNOLOGY
Göteborg, Sweden, 2005

Fluidized-Bed Reactor Systems
for Chemical-Looping Combustion
with Inherent Separation of CO_2

EVA JOHANSSON
ISBN 91-7291-685-0

Doktorsavhandlingar vid Chalmers tekniska högskola
Ny serie nr 2367
ISSN 0346-718X

Department of Energy and Environment
Division of Energy Technology
Chalmers University of Technology

SE-412 96 Göteborg
Sweden

Telephone +46 (0)31 7721000

Cover: Investigation of carbon dioxide capture in the hot 300 W reactor.

Printed in Sweden
[Reproservice, Chalmers University of Technology]
Göteborg, 2005

Fluidized-Bed Reactor Systems for Chemical-Looping Combustion with Inherent Separation of CO_2

EVA JOHANSSON

Department of Energy and Environment
Division of Energy Technology
Chalmers University of Technology

Abstract

In chemical-looping combustion (CLC) a gaseous fuel can be burnt with inherent separation of carbon dioxide. The system consists of two reactors, a fuel reactor and an air reactor and an oxygen-carrier in the form of metal oxide particles that transports oxygen from the air to the fuel. The gas leaving the air reactor consists of nitrogen and unreacted oxygen, while the gas from the fuel reactor consists of water and carbon dioxide. The water can easily be condensed, and the remaining carbon dioxide can be liquefied for subsequent storage.

A CLC reactor system can be designed with two interconnected fluidized beds. Two types of cold-flow models of CLC systems and one 300 W_{th} chemical-looping combustor have been designed and constructed, and tested with respect to parameters which are important for CLC. The first design is similar to a circulating fluidized bed, with an extra bubbling bed added on the return side. This bubbling bed is the fuel reactor and the riser is the air reactor. The main purpose of testing the reactor was to establish suitable operating conditions as well as testing the influence of bed mass and fluidization velocities on solids circulation flux and gas leakage. The second design is a two-compartment reactor, where a downcomer transports particles from the air reactor to the fuel reactor, and a slot in the bottom of the wall between the reactors leads the particles back to the air reactor. The second design was used both for a cold-flow model and the 300 W_{th} chemical-looping combustor.

Both cold-flow models indicated that the solids circulation rate between air and fuel reactor was high enough for CLC, and that leakage was small and could be lowered even more with simple countermeasures. The second design was also successfully tested with combustion of natural gas and syngas in the temperature range 800-950˚C, using two different nickel based oxygen-carriers. One oxygen-carrier was tested with syngas, and the conversion of the fuel was high, often exceeding 99%, with hydrogen and carbon monoxide concentrations close to thermodynamic equilibrium. For natural gas, high conversion of the fuel was found for both oxygen-carriers, also around 99%. One of the particles tested was in operation for 150 h, of which 30 h with combustion, the other particle for 18 h, of which 8 h with combustion. No loss in reactivity was observed during testing and virtually no attrition of the two particles was detected.

Keywords: Chemical-Looping Combustion, Interconnected Fluidized Beds, Carbon Dioxide Capture.

The thesis is based on the following papers:

I. Johansson, E., A. Lyngfelt, T. Mattisson and F. Johnsson. A Circulating Fluidized Bed Combustor System with Inherent CO_2 Separation –Application of Chemical Looping Combustion, in J.R. Grace, J. Zhu and H. de Lasa (ed.) *Seventh International Conference on Circulating Fluidized bed*, Niagara Falls, Canada, 2002, pp. 717-724

II. Johansson, E., A. Lyngfelt, T. Mattisson and F. Johnsson. *Gas Leakage Measurements in a Cold Model of an Interconnected Fluidized Bed for Chemical-Looping Combustion*, Powder Technology 134 (2003) pp. 210-217

III. Johansson, E., B. Kronberger, G. Löffler, T. Mattisson, A. Lyngfelt, H. Hofbauer. A Two-Compartment Fluidized Bed for Chemical-Looping Combustion –Design and Experiments, *Seventh International Conference on Energy for a Clean Environment*, Lisbon, Portugal, 2003

IV. Kronberger, B., E. Johansson, G. Löffler, T. Mattisson, A. Lyngfelt, H. Hofbauer. *A Two-Compartment Fluidized Bed Reactor for CO_2 Capture by Chemical-Looping Combustion* Chemical Engineering and Technology 27 (2004) pp. 1318-1326

V. Johansson, E., T. Mattisson, A. Lyngfelt and H. Thunman. *A 300 W Laboratory Reactor System for Chemical-Looping Combustion with Particle Circulation*, submitted for publication

VI. Johansson, E., T. Mattisson, A. Lyngfelt and H. Thunman. *Combustion of Syngas and Natural Gas in a 300 W Chemical-Looping Combustor*, submitted for publication

TABLE OF CONTENTS

ACKNOWLEDGEMENT

I would like to express my gratitude to all the persons who in one way or another contributed to this thesis. I particular, I would like to thank:

My supervisor Professor Anders Lyngfelt for providing me the opportunity to work in this interesting field and accomplish this thesis work. As well, I would like to thank him for his interest in my work, his availability and encouragement.

My supervisor Associate Professor Tobias Mattisson for valuable discussions, encouragement and experimental suggestions.

All colleagues in the chemical-looping group at Chalmers and in the CCCC-project. Paul Cho for valuable discussions not always concerning chemical-looping combustion, Marcus Johansson for the graphs provided to me even though I did not always know what I wanted and Magnus Rydén for creative new ideas like “ebonit-katt-kraftverket”. I would also like to mention Professor Filip Johnsson, dr Bernhard Kronberger and Hilmer Thunman.

Lennart Darell, Niklas Hansson at VTS and Ulrik Rosen at 7rs Mekaniska for help with the experimental devices.

All the colleagues that are or have been working at the department during these years for providing a friendly and inspiring environment. I would like to mention Ulrika Claeson-Colpier, Jenny Sahlin, Anna Krook and of course all participants in the “ten-o’clock coffee group”.

Financial support from Miljösektionen, the project CCCC Capture of CO_2 in Coal Combustion (ECSE contract No 7220-PR-125) and the Swedish Energy Agency.

Family and friends for all the things that really matters. Special thanks to Magnus and our lovely son Oskar.

To Magnus and Oskar

"Without changing our pattern of thought,
we will not be able to solve the problems we
created with our current patterns of thought"
/Albert Einstein

Chapter 1

1 INTRODUCTION

This thesis treats a technique for separation of carbon dioxide in combustion of fossil fuels. Carbon dioxide is a greenhouse gas, and about 75% of the anthropogenic release of carbon dioxide comes from combustion of fossil fuels, (IPCC 2001). It is generally accepted that greenhouse gases contribute to the increased global temperature. In order to stabilize the atmospheric concentration of CO_2, substantial measures are necessary quickly. At present, renewable energy sources with moderate costs, such as wind energy and biomass, seem to have a limited potential for substitution of fossil energy (Strömberg 2001). One possibility to decrease the CO_2 emissions is to capture and dispose of the carbon dioxide from fossil fuels.

After a short summary of the greenhouse effect and an introduction to different techniques for separating carbon dioxide, this thesis will focus on one of these techniques, chemical-looping combustion.

1.1 The greenhouse effect and CO_2 mitigation

There are indications of an increased global average temperature during the last century. Increasing temperature can give several different effects, such as increase of the sea water level, agriculture and fisheries may be disrupted, and the prevalence of diseases such as malaria may increase. Also ecological systems will be influenced. A change in the temperature disturbs the ecological equilibrium, affecting location of ecological systems and the mix of species that they contain. The faster the change, the greater the disequilibria may be, and the harder it will be for ecosystems to adapt.

The concentration of CO_2 in the atmosphere has increased from 280 to 350 ppm since the industrialization. Measurements have shown that the global annual average temperature has increased 0.6°C ± 0.2°C during the last century, (IPCC 2001). Greenhouse gases absorb long wave radiation and contribute to the global warming. Carbon dioxide is the gas that contributes the most, about 55%, when both concentration and absorption are taken into account, (Harvey 2000). Carbon dioxide has the lowest relative heat trapping ability of the greenhouse gases, but the amount of carbon dioxide emitted is much larger than other greenhouse gases. The climate sensitivity is about 2.5°C for a doubling of the carbon dioxide concentration in the atmosphere (Azar and Rodhe 1997). This value is uncertain and may vary in the range of 1.5-4.5°C due to feedbacks such as change in water vapour concentration, clouds and ice cover. If the emission of greenhouse gases continues to increase at the present rate, the temperature may change about 0.3 degrees per decade (Davis 1986). The rates of change in temperature may be greater than the time necessary for ecological systems to adapt. The greater the rate and extent of the change, the higher is the probability of substantial ecosystem disruption and species extinction (IPCC 1998). For example the greatest documented movement for trees are in average 20-25 km per century, which in the Great Lakes USA region corresponds to a temperature increase of about 0.2-0.25 degrees per century (Davis 1986).

Warmer climate causes a movement of the vegetation belts polewards and upwards in altitude to compensate for the temperature increase. The moving vegetation can be limited by inadequate light, oceans, seas, mountains and poor soil (IPCC 1998; Walther et al. 2002). Also human activities, such as farming, prevent vegetation from movement. The nutrient limits for different species differ; e.g. deciduous forests have a high need of mineral nutrient while conifer forests live where the amount of mineral nutrients in the soil are poor.

Climate changes affect the ecosystems directly, and also in indirect ways, e.g., changes in soil moisture. Inputs to soil water are rain and snowmelt; outputs are evapotranspiration, direct evaporation from bare soils and subsurface drainage. An increase in air temperature will evaporate more water from the soil and thereby dry the soil. However, it is likely that changes in temperature profiles will change the

structure of precipitation. Climate models suggest that days with heavy rainfall are likely to increase, even in areas where the yearly total amount of precipitation is the same or less, (Harvey 2000). More intense rain means more water during a shorter time. Since the runoff from soil increases with the moisture content, more of the total rainfall will run off, causing even higher reduction in soil moisture.

An observed rise in sea level is due to temperature increase, but there are also other minor anthropogenic effects (permanent removal of water from aquifers, loss in soil moisture because of deforestation and reduction in the extent of wetlands among others). A temperature increase causes melting of glaciers and other ice masses, and also a thermal expansion of the ocean water (Harvey 2000).

Although the specific effects, e.g. local temperature changes and changes in rain and dry periods, of an increased concentration of CO_2 in the atmosphere are uncertain, it is clear that the ecological systems will be affected. It is therefore of great importance to stabilize the atmospheric concentration of greenhouse gases, especially CO_2. This means that a drastic reduction in the release of CO_2 from combustion of fossil fuels is necessary. This could be achieved by:

- Increased efficiency in conversion and use of energy.
- Change to fuels with lower carbon content, i.e. that emits less CO_2 per unit of useful energy.
- Increased utilization of renewable energy sources.
- Increased utilization of nuclear power.
- Increased sequestration of carbon dioxide by natural sinks that is the terrestrial biosphere.
- Capture and sequestration of carbon dioxide from energy plants and other sources.
- Decreased energy consumption per capita

In a world where the energy demand is expected to increase with growth in economy it is not likely that any one of these measures in itself will be enough, but rather a combination of these. In this thesis a technology for capture of CO_2 called chemical-looping combustion (CLC) has been investigated.

1.2 CO_2 separation and sequestration

To achieve a slightly concentrated stream of carbon dioxide several methods can be used. These techniques are normally divided into three principal groups.

- Post combustion
- Pre combustion
- O_2/CO_2 combustion ("oxy fuel ")

Chemical-Looping Combustion, which is a combustion technique with inherent separation of CO_2, does not fit into either of these groups. It would best fit in a fourth category, i.e.:

- Unmixed combustion.

The different techniques will be briefly presented below.

1.2.1 Post-combustion

In post combustion capture, the carbon dioxide is separated from the flue gas, Figure 1. This means that the combustion process itself is not affected, but the separation step needs energy, and this energy is taken from the combustion step, which lowers the energy efficiency of the process.

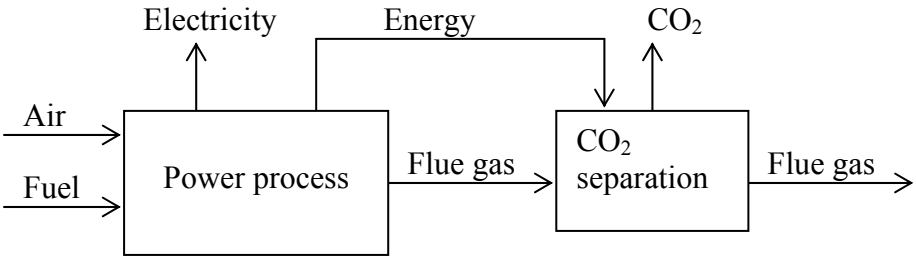

Figure 1. *Post-combustion principle*

The separation step can be an absorption/desorption process with for example monoethylene amine (MEA) as absorber. In this case the flue gas is led through an absorption tower, where an absorber (MEA) absorbs the carbon dioxide. The rest of the flue gas is released to the atmosphere, while the CO_2-rich absorber is led into a CO_2 stripper tower, where CO_2 is released, and the MEA is then recycled back into the absorption tower. The technology is commercially available and has been used for various applications since the late seventies.

Other possibilities for the CO_2 separation step are adsorption, membrane separation and regenerable solid solvent.

1.2.2 Pre-combustion

The idea is to convert the fuel to CO_2 and H_2 and to separate the CO_2 before the combustion, Figure 2. The first step is to convert the fuel to a suitable gas containing CO, CO_2, H_2 and H_2O by partial oxidation, reforming or a combination of these. In the second step CO and H_2O are shifted to CO_2 and H_2. Thereafter, the carbon dioxide is removed from the gas mixture. This is done for example by using absorption. Because the concentration of carbon dioxide is quite high the gas separation step is cheaper compared to post-combustion where a stream highly diluted with nitrogen needs to be treated. The remaining hydrogen can be used for instance in fuel cells or a combined gas turbine cycle.

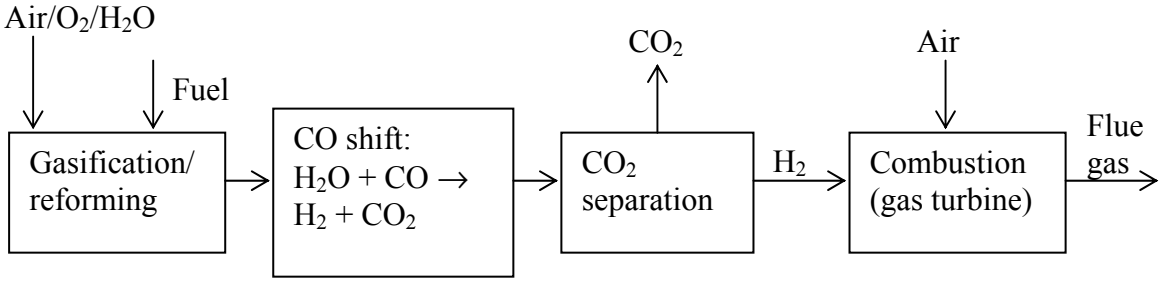

Figure 2. *Pre-combustion principle, also called CO-shift.*

1.2.3 O_2/CO_2-combustion (oxy fuel)

The oxy-fuel principle is shown in Figure 3. The combustion of the fuel is accomplished with a mixture of oxygen and recirculated carbon dioxide instead of air. Before the combustion chamber, a unit separating oxygen from the air is needed. Since no nitrogen is present, the flue gas will consist of carbon dioxide, water and some argon. The argon is present since it follows the oxygen and not the nitrogen in the air separation process. After the combustion a flue gas treatment, involving condensing and removal of water and removal of non-condensable gases, the carbon dioxide is received pure. Some of the carbon dioxide is circulated to the combustion chamber because of difficulties of using pure oxygen in combustion.

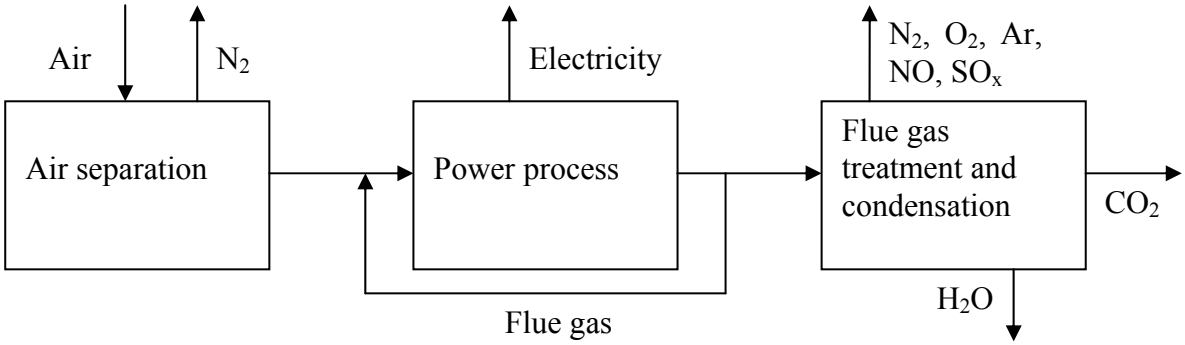

Figure 3. *Oxy-fuel principle*

1.2.4 Unmixed combustion

There are some combustion methods where the combustion air and the fuel never are mixed, and therefore the carbon dioxide is inherently separated during combustion, without using any gas separation step. Examples of unmixed combustion are fuel cells, AZEP and chemical-looping combustion.

In a fuel cell chemical energy is converted to electrical energy. A special type of fuel cell can be used to produce electricity and separate oxygen from air. First, the hydrocarbon fuel has to be converted to CO and H_2 at the anode. Thereafter these products are oxidized to CO_2 and H_2O by oxygen ions that diffuse through the electrolyte from the cathode. Since the electrolyte is selective and only transports oxygen, the carbon dioxide and water are received pure.

AZEP, Advanced Zero Emissions Power Plant, is a technology where O_2 is transferred from the combustion air through a membrane in the combustion reactor. Then, the combustion takes place in a nitrogen free environment, and the flue gas consists of carbon dioxide and water. The reactor is integrated in a gas turbine (Sundkvist et al. 2001).

Chemical-looping combustion is a combustion method with inherent separation of carbon dioxide. The air is never mixed with the fuel, two flue gas streams leave the system, one with the reaction products and one with nitrogen and some oxygen from the air. The technique will be explained in the next chapter.

1.3 Scope of the thesis

The aim of the thesis is to investigate possible designs of chemical-looping combustion reactors. The dissertation is based on six papers. The first four papers present two different designs of a chemical-looping system, and tests made in cold-flow models. The last two papers show results from a 300 W chemical-looping combustor based on the optimised design in papers III and IV.

2 CHEMICAL-LOOPING COMBUSTION (CLC)

Chemical-looping combustion (CLC) differs from the above-mentioned techniques for CO_2 capture by separating the carbon dioxide during combustion. The combustion system consists of two reactors, a fuel reactor and an air reactor, and an oxygen-carrier that transports the oxygen from the air to the fuel, see Figure 4. In this way the fuel and air are never mixed, and the product gas from the fuel reactor consists of carbon dioxide and water, while the nitrogen and excess oxygen leaves the process in a separate gas stream from the air reactor. The water can be condensed and the remaining carbon dioxide compressed for storage.

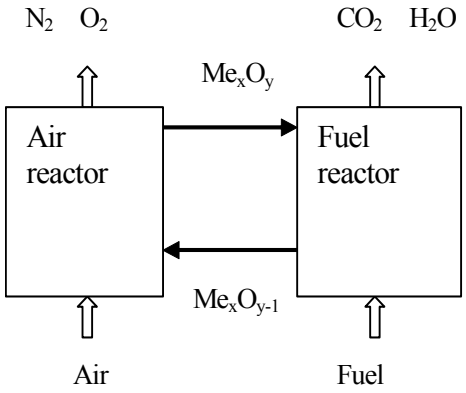

Figure 4. *Chemical-looping combustion*

In the fuel reactor, the oxygen-carrier reacts with the gaseous fuel, according to reaction (1):

$$(2n+m)Me_xO_y + C_nH_{2m} \rightarrow (2n+m)Me_xO_{y-1} + mH_2O + nCO_2 \quad (1)$$

The reduced oxygen-carrier is transported to the air reactor where it is oxidized by the oxygen in the incoming air.

$$Me_xO_{y-1} + ½O_2 \rightarrow Me_xO_y \quad (2)$$

The total reaction is the sum of reactions (1) and (2), and the same as for normal combustion in air.

$$C_nH_{2m} + (n+m/2)O_2 \rightarrow mH_2O + nCO_2 \quad (3)$$

Thus, the oxygen-carrier is oxidized back to the original metal oxide, and can be returned to the fuel reactor for a new cycle. Possible metal oxides which could be used in a chemical-looping combustor are some oxides of common transition-state metals, such as iron, nickel, copper and manganese, (Cho 2005). Reaction (1) is exothermic with subsequent heat release, while reaction (2) may be endothermic or exothermic, depending on oxygen-carrier and fuel. However, the total heat released is the same as for conventional combustion when oxygen and fuel are in direct contact.

In this work reactor systems of interconnected fluidized beds are investigated for chemical-looping combustion. Below a background for this work is given. First, some important criteria for a chemical-looping combustion reactor system are discussed in section 2.1. Second, some fundamental relations for chemical-looping combustion will be given in section 2.2, followed by an introduction to fluidization, 2.3. Work on chemical-looping combustion has been focused on three areas, thermodynamic studies of the process, development and tests of oxygen-carriers and development and tests of reactor designs. Overviews of these areas are presented in sections 2.4, 2.5 and 2.6 respectively.

2.1 Reactor system

Important criteria for the CLC system are:

i) The rate of circulation of oxygen-carrier between the reactors needs to be sufficient to transport the amount of oxygen needed for the combustion of the fuel. For the case of endothermic reaction in the fuel reactor the circulation also needs to be sufficient for maintaining an adequate temperature in the fuel reactor.

ii) The amount of bed material in both of the reactors has to be adequate for sufficient conversion of gas.

iii) The gas leakage between the two reactors must be minimized to prevent the carbon dioxide from being diluted with nitrogen, which will increase the power needed to liquefy the CO_2, or to prevent carbon dioxide from leaking to the air reactor decreasing the efficiency of carbon dioxide capture.

In this work interconnected fluidized beds were chosen for the design of the CLC system, and the oxygen-carrier acts as bed material. Fluidized beds are suitable since in fluidization there is a large contact area between gaseous and solid phase, and proven technology is also available for moving particles between reactors.

The reasons why these three different criteria are important for a CLC reactor system are further discussed below.

2.1.1 Net solids flux

The needed solids circulation is determined by two factors. The first is the oxygen needed for combustion. Since the particles are carrying the oxygen for the combustion reaction, the net solids flux between the reactors has to be high enough to transfer the needed amount of oxygen. The second is the heat. The reaction in the air reactor is exothermic, but the reaction in the fuel reactor is often endothermic. For the case when the reaction in the fuel reactor is endothermic, the particles are not only transferring the oxygen but also the heat to reach sufficient temperature in the fuel reactor.

2.1.2 Bed material

The amounts of bed material in the air and fuel reactors are dependent on the rate of the reaction between the gas and the oxygen-carrier, i.e. for a slow reaction more material is needed

2.1.3 Gas leakage

The gas leakage between the reactors has to be minimized. If there is a leakage from the fuel reactor into the air reactor, the carbon dioxide capture efficiency will decrease since carbon dioxide will escape into the atmosphere. A leakage in the other direction, i.e. from the air reactor to the fuel reactor, will cause the carbon dioxide stream to be diluted with nitrogen, and extra costs for purification of CO_2 might be incurred.

2.2 Theory

The heat released at combustion with an oxygen-carrier is the same as for conventional combustion. Below some fundamental relations relevant for chemical-looping combustion are given. They have been presented previously by for instance Lyngfelt et al. (2001). Assuming total combustion of a fuel with heat value of H_i, and the thermal power, P_{th}, the mass flow of fuel is given by:

$$\dot{m}_{fuel} = \frac{P_{th}}{H_i} \tag{4}$$

The oxygen needed is given from the stoichiometric combustion of the fuel:

$$\dot{m}_o = M_{O_2} \cdot \frac{\dot{m}_{fuel}}{M_{fuel}} \cdot S_r \tag{5}$$

Where S_r is the stoichiometric ratio between oxygen and fuel, M is the molar mass for oxygen and fuel respectively. With combustion an excess of air is needed to make sure that all fuel is burnt out. This excess air ratio, λ, is the ratio between air actually added and stoichiometric needed air. The air mass flow is then given by:

$$\dot{m}_{air} = \frac{\dot{m}_o}{M_{O_2} \cdot 0.21} \cdot \lambda \cdot M_{air} \tag{6}$$

The cross-section area, A, of both reactors is determined from the gas flow and the velocity chosen.

$$A = \frac{\dot{m}}{\rho \cdot u} \tag{7}$$

Where ρ is the density of the gas at the actual temperature in the reactor and u is the velocity. The velocity is chosen to obtain suitable fluidization conditions.

The degree of oxidation, or conversion, of an oxygen-carrier is defined as:

$$X = \frac{m - m_{red}}{m_{ox} - m_{red}} \tag{8}$$

where m is the actual mass of the oxygen-carrier, m_{ox} is the mass of the oxygen-carrier when fully oxidized, m_{red} is the mass of the oxygen-carrier when fully reduced. Since oxygen is transferred from the air reactor to the fuel reactor, the conversion is higher in the air reactor than in the fuel reactor, and the difference in conversion, ΔX, is:

$$\Delta X = X_{ox} - X_{red} \tag{9}$$

The oxygen ratio, R_o, is the mass fraction of oxygen that can be used in he oxygen transfer. It shows the maximum oxygen that can be transported from the air reactor to the fuel reactor. It is defined as:

$$R_o = \frac{m_{ox} - m_{red}}{m_{ox}} \tag{10}$$

A mass-conversion based on the mass of the oxygen-carrier is defined as:

$$\omega = \frac{m}{m_{ox}} = 1 + R_o(X - 1) \tag{11}$$

The rate of circulation of oxygen-carrier based on oxygen transfer between the reactors can be calculated from:

$$\dot{m}_{sol} = \frac{\omega_{air} \cdot \dot{m}_o}{\Delta\omega} \approx \frac{\dot{m}_o}{\Delta X \cdot R_o} \tag{12}$$

The amount of oxygen-carrier needed in each reactor is inversely proportional to the reactivity of the oxygen-carrier and can be calculated from:

$$m_{bed} = \frac{\omega \cdot \dot{m}_o}{d\omega / dt} \tag{13}$$

2.3 Fluidization

Fluidization is a technique where a bed of solids (particles) is exposed to an upward stream of fluid (gas or liquid) and behaves like a fluid. To obtain fluidization, the gas velocity must exceed the minimum fluidization velocity, u_{mf}, which occurs when the pressure drop caused by friction between solids and gas becomes equal with the weight of the bed. Required gas velocity depends on the properties of the gas and particle. The pressure drop over the bed becomes constant even when the gas velocity exceeds the minimum fluidization velocity. This is because excess gas leaves the bed in bubbles, and therefore the particles do not experience a gas velocity higher than u_{mf}. This region is called bubbling fluidization.

The terminal velocity, u_t, is reached when the drag force is equal with the weight of a single particle. When the gas velocity exceeds the terminal velocity, the particles can be carried away from the bed by the gas. A fluidized bed operated at velocities above the terminal velocity will have a dense bottom bed, and above this a suspension of particles. The particle concentration is decreases with the height of the vessel.

2.4 The chemical-looping process

The chemical-looping combustion process was first presented by Richter and Knoche (1983). Later, the process was named chemical-looping combustion (Ishida et al. 1987). When the process was first introduced, the main objective was to increase the overall thermal power plant efficiency. Now, the main objective is on carbon dioxide capture.

Thermodynamic studies have been focused on comparative studies of thermal power processed with chemical-looping combustion, and often including exergy analysis of chemical-looping combustion. This has been addressed by research groups at Dartmouth College (Harvey 1994), at Tokyo Institute of Technology, e.g. (Ishida and Jin 1994), Royal Institute of Technology e.g. (Anheden et al. 1995; Anheden and

Svedberg 1996; Wolf 2004), at Norwegian University of Science and Technology (Naqvi et al. 2004; Brandvoll 2005), at University of Genoa (Bisio et al. 1998), at Louisiana State University (Yu et al. 2003) and at Politecnico di Milano (Consonni and Vigano 2005). The main focus has been on pressurized systems with combined cycles, and generally, the studies show high efficiencies for chemical-looping combustion. The efficiencies presented are equal or even higher than conventional technology, with the benefit of carbon dioxide capture. Note that this work is theoretical and not based on verified performance of actual oxygen-carriers, for example being able to sustain high temperatures. Nevertheless, the studies show that the potential for chemical-looping combustion is high. They also provide requirements on temperatures and pressure for optimization of the efficiency.

2.5 Oxygen-carriers

There are some important criteria for the oxygen-carrier. The rate of oxidation and reduction has to be sufficient. Otherwise the amount of oxygen-carrier needed in the two reactors would be too large. Also the oxygen carrying capacity needs to be sufficient. This is to avoid the circulation of particles between the reactors from being very large. Since the proposed reactor system consists of fluidized beds, the particles need to have good strength, and low tendency for fragmentation and attrition. They also need to have a low tendency for agglomeration at the high temperatures used. There are also other aspects than chemical and physical, such as the cost of the oxygen-carrier, and environmental and health issues.

A few authors have presented reactivity data from tests with pure metal oxides, such as iron ore, e.g. (Mattisson et al. 2001). However, most studies have been conducted with metal oxides which are combined with an inert material. This gives the oxygen-carrier a more porous structure, and thereby increases the surface area for reaction. It may also increase the mechanical strength and attrition resistance, (Adánez et al. 2004).

Table 1. *The oxygen ratio, R_o, eq (10), for different metal oxides.*

Me_xO_y/Me_xO_{y-1}	R_o
NiO/Ni	0.21
CuO/Cu	0.20
Mn_3O_4/MnO	0.07
Fe_2O_3/Fe_3O_4	0.03

Different oxygen-carrier particles have been tested, and a number of publications related to the development of oxygen-carrier particles have been issued by different research groups at Tokyo Institute of Technology, e.g. (Jin et al. 1999; Ishida et al. 2002), Chalmers University of Technology, e.g. (Cho et al. 2004; Mattisson et al. 2004), Korea Institute of Energy Research, e.g. (Song et al. 2003), TDA Inc, e.g. (Copeland et al. 2001), CSIC-ICB in Zaragoza, e.g. (Adánez et al. 2004), National Institute for Resources and Environment in Japan, (Hatanaka et al. 1997), Politecnico di Milano (Villa et al. 2003) and Norwegian University of Science and Technology (Brandvoll 2005). An overview of the work which has been performed on different oxygen-carriers can be found in theses by Cho (2005) and Brandvoll (2005). In general, particles tested have active oxides of Fe, Ni, Cu or Mn as active part, combined with some type of inert carriers, such as Al_2O_3, ZrO_2, TiO_2 or MgO. The amount of oxygen which can be transferred between the reactors is dependent on the metal oxide system used, and can be seen by the oxygen-carrier ratio, R_o, for the most common metal oxides, see Table 1. It should be noted that the table presents the oxygen ratio for the pure metal oxides, and the oxygen ratio would be lower when inert material is added. There are also thermodynamic limitations which should be considered. Fe, Cu and Mn have oxide systems which have the ability to fully convert methane and syngas completely to CO_2 and H_2O, but for Ni there is a thermodynamic limit of 99-99.5%. This will be discussed later. The reactivity under alternatively oxidising and reducing conditions can vary greatly between different oxygen-carriers, and is a function of the metal oxide and inert used, the preparation method and temperature during heat treatment. In general, NiO has been found to be the most reactive oxygen-carrier with methane, although well suited particles based on Cu, Mn and Fe have also been developed, e.g. (Adánez et al. 2004; Johansson et al. 2005). Only limited experimental studies have been performed with syngas as fuel.

2.5.1 Environmental and health aspects of oxygen-carriers

The availability of the proposed materials for oxygen-carriers differs. Iron is after alumina the most common metal, and the fourth most common element on earth. Also manganese is common, while copper and nickel exist in lower concentration. To compare, the mineable reserve of iron is estimated to be 110000 million tons, while for nickel it is 60 million tons, (NE 2005). In general, the environmental impact of mining a metal that exists in high concentration is smaller than mining a rare metal.

After use in a chemical-looping combustor, it is a possibility that the oxygen-carrier material could be recycled and used for other purposes instead of being treated as waste. Also, it might be a possibility to use waste products from the industry, e.g. steel industry, to produce oxygen-carriers for chemical-looping combustion.

Also with respect to health aspects the metals differ from each other. For instance iron has a very low toxicity, whereas nickel is the unhealthiest metal of the proposed ones. The latter can cause contact allergy and inhalation of nickel dust may cause chronic respiratory infections and asthma like conditions. Also the olfactory sense can be damaged and it may cause cancer in lung and sinus. Copper and manganese can also have adverse effects. Serious poisoning of copper is unusual since the uptake from the intestine is low, but inhalation of metal smoke containing copper can give metal ague/shiver, with respiratory irritation, cough and fever. Exposure of manganese can cause damages on the lungs and neurological disorders. (NE 2005). Although long term exposure of some of these metals or metal oxides may cause health problems, all are handled and used in large scale industrial applications. Furthermore, chemical-looping combustion is expected to be used in a system with highly efficient separation of particles.

2.6 Interconnected fluidized beds

For chemical-looping combustion two inter-connected reactors are needed. Various systems of interconnected fluidized beds are in actual use for various applications or have been proposed in the literature. Below some systems are discussed as background for understanding possible choices for actual full-scale plants but also as

options for systems suitable for use in laboratory. First two designs considered as laboratory chemical-looping combustors are presented. The second design was chosen and built both as cold-flow model and chemical-looping combustor. Thereafter, systems of possible relevance for design of a full-scale plant are discussed.

A four-compartment reactor was first proposed by Kuramoto et al., (1986), to be used for gasification of biomass and municipal waste, and it has been further investigated by others, (Fox et al. 1989; Snip et al. 1996; Abellon et al. 1997; Snieders et al. 1999) This reactor consists of two slow fluidized beds and two more vigorously fluidized beds. Overflows lead the particles from the fast to the slow beds, and orifices in the bottom of the wall leads the particles from the slow to the fast beds. In this way the particles circulate between the four reactors.

Chong et al. (1986) presented a two-compartment reactor for oil shale retort, and this reactor has been further investigated by He et. al. (1993) and Fang et al., (2003). This reactor system has a vigorously fluidized bed connected to a slow fluidized bed. The particles follow the gas in the vigorously fluidized bed, and fall down into a downcomer between the beds, and are transported into the slow bed. The pressure induced by the particle column in the downcomer forces particles into the slow bed, raising the pressure drop of this. Thus, the pressure drop in the slow bed becomes higher than in the other bed, and therefore the particles are pressed back into the fast bed through an orifice in the lower part of the wall between the beds.

Fluid catalytic cracking (FCC) was developed in the 1940s and was the beginning of modern fluidization technology, (Avidan and Shinnar 1990). Now it is the most common application of interconnected fluidized beds (Avidan 1997). There are different designs for FCC, but they consist of a regenerator and a reactor. There is a circulation of particles between these two fluidized beds, often consisting of an outlet in the bottom of the bed, and pneumatic transport through a tube to the other fluidized bed. Depending on the cracker design, there may also be solids circulation loops within the regenerator and reactor. The technology is very specific for cracking, and the temperatures used are lower than those needed for chemical-looping.

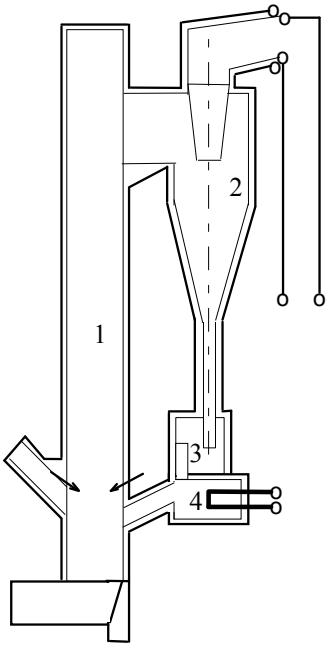

Figure 5. *A CFB-boiler. 1) riser, 2) cyclone, 3) particle seal, 4) fluidized bed heat exchanger.*

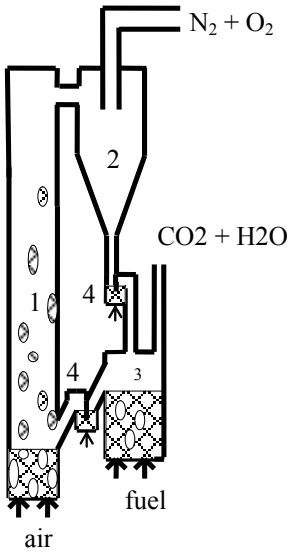

Figure 6. *Layout of a chemical-looping combustor, with two interconnected fluidized beds. 1) air reactor, 2) cyclone, 3) fuel reactor, 4) particle seals.*

A proven technology for combustion of solid fuels is circulating fluidized bed boilers. The first circulating fluidized bed (CFB) boiler was built in the end of 1970s. Today, CFB boilers of the size 550 MW_{th} are in use. A circulating fluidized bed boiler is operated at velocities above the terminal velocity in the riser and has equipment, e.g. a cyclone, to return the particles back to the bed, see Figure 5. Often the CFB boiler has a small bubbling fluidized bed which the particles pass before returning to the riser. This is used for extracting heat from the process and is called fluidized bed heat exchanger. The CFB boiler operates in about the same temperature range as CLC, and with minor modifications, a CFB boiler could be converted to a chemical-looping combustor, (Morin and Béal 2005). The riser is used as air reactor, and after the cyclone, a bubbling bed is added as fuel reactor. A chemical-looping combustor with this design was proposed by Lyngfelt et al. (2001), Figure 6. The important difference compared to the CFB boiler in Figure 5, is that the fluidized bed heat exchanger is exchanged for a fuel reactor and that an additional particle seal is added.

A similar system, a circulating fluidized bed for gasification of biomass was built and tested as cold-flow model (Kehlenbeck et al. 2001) and also a 100 kW_{th} steam gasifier was built, (Pfeifer et al. 2004). The gasification system consists of a gasification reactor and a combustion reactor, and using nickel-enriched catalytic particles as bed material. The combustion reactor is a riser ending in a bubbling fluidized bed. In the bottom of this bubbling bed a downcomer leads the particles to the gasification reactor, a bubbling fluidized bed, and from the bottom of this reactor, the particles are led back into the riser. The gasification reactor is fluidized with steam, and the combustion reactor with air, and the flue gases leaves the system separately. In this way, the product gas is free of nitrogen.

In addition to the system presented in this work, two chemical-looping combustors have been presented in the literature, a 10 kW unit at Chalmers University of Technology (Lyngfelt et al. 2004; Lyngfelt and Thunman 2005) and a 50 kW unit at Korea Institute of energy Research (Ryu et al. 2004). The 10 kW unit has the principal design shown in Figure 6, and it was first tested as a cold-flow model at Vienna University by Kronberger et al. (Kronberger et al. 2005). Stable and suitable operating conditions were identified. In the 10 kW chemical-looping combustor, an oxygen-carrier based on nickel oxide was operated for 100 h with natural gas as fuel. A fuel conversion efficiency of 99.5% was achieved, and no carbon dioxide escaped to the air reactor, hence, all carbon dioxide was captured in the process. Only small losses of fines were observed. The 50 kW chemical-looping combustor was operated with methane as fuel and two types of oxygen-carriers. A nickel oxide oxygen-carrier was tested during 3.5 h and a cobalt oxide was tested during 25 h. For the nickel oxide oxygen-carrier, the concentration based on dry flue gases of CO_2 leaving the fuel reactor was 98% and for cobalt oxide 97%. The two units have a similar design, but differ at the return from the fuel reactor. In the 10 kW unit the particles leave the fuel reactor through an overflow, i.e. the bed height in the fuel reactor is always constant, while in the 50 kW unit the particles leave the fuel reactor from the bottom of the bed, and the particle flow i.e. the bed height of the fuel reactor, is controlled by an L-valve.

Chapter 3

3 EXPERIMENTAL

Prior to this work, only limited work had been conducted with respect to chemical-looping combustion, and that work was almost entirely focused on development of oxygen-carrier particles. Thus, there was a need to investigate reactor designs.

Three fluidized units for chemical-looping combustion were designed and constructed; two cold-flow models and one 300 W chemical-looping combustor. The main purpose with the first cold-flow unit to investigate a possible design for a pilot reactor. The chosen design was similar to a circulating fluidized bed, but with a bubbling fluidized bed on the return from the cyclone.

Oxygen-carriers had earlier been tested in batch reactors, but there was a need for a continuously operating small size chemical-looping combustor to i) study the process and ii) test oxygen particles in real chemical-looping combustion. A simpler design than the CFB-like reactor tested above was preferred, and a two-chamber fluidized bed was chosen, first proposed by Chong et al. (1986). A laboratory chemical-looping combustion reactor system with a thermal power of 100-300 W was designed, and first a cold-flow model was built and tested. The testing in the cold-flow model indicated that the design was suitable and subsequently the 300 W chemical-looping combustor was built with only some minor modifications. In this unit it was possible to demonstrate the process and test performance of oxygen-carrier particles in extended operation using both syngas and natural gas as fuel.

A cold-flow model has some benefits compared to a hot unit, and therefore it is an advantage to first construct and study a cold-flow model. They are cheaper, easier to

handle and allow visual observation of flow structures. Pressure profiles, solids circulation data, gas leakage between the reactors are parameters that can be predicted for a hot unit by studies in a cold-flow model.

The two cold-flow models were built and operated according to the simplified scaling laws for fluid dynamics proposed by Glicksman et al (Glicksman et al. 1993). The following dimensionless numbers are kept constant during scaling:

$$\frac{u_0^2}{g \cdot L}, \frac{\rho_s}{\rho_f}, \frac{u_0}{u_{mf}}, \frac{G_s}{\rho_s \cdot u_0}, \textit{Bed Geometry, } \phi\textit{, Particle size distribution} \quad (14)$$

where u_0 is the superficial gas velocity, u_{mf} is the minimum gas velocity, g is the acceleration due to gravity, L is the characteristic length in the system, G_s is the solids circulation rate, ϕ the particle coefficient, and ρ_s and ρ_f is the density of the solids and the fluid respectively. Design calculations concerning fluidization were made according to Kunii and Levenspiel (1991).

3.1 Chosen designs and experimental set-ups

3.1.1 The CFB-like model (Papers I-II)

The design of the cold-flow model used in papers 1-2 is shown in Figure 7. The reactor configuration is similar to a circulating fluidized bed (CFB), but with the addition of a bubbling fluidized bed on the solids return side. This design is chosen since it is simple and there is long experience on CFBs for combustion of solid fuels. The bubbling bed (3), which is situated below the downcomer from the cyclone, acts as the fuel reactor where oxygen is transferred from the particles to the gaseous fuel. An overflow leads the reduced oxygen-carriers to the riser (1) that acts as the air reactor where the previously reduced metal oxide is regenerated. Two particle seals prevent gas mixing between the two reactors: one pot-seal in position (5) and one at the bottom of the downcomer from the cyclone. This means that the fuel reactor also has the function of a particle seal. The actual model was constructed in Perspex and is shown in Figure 8.

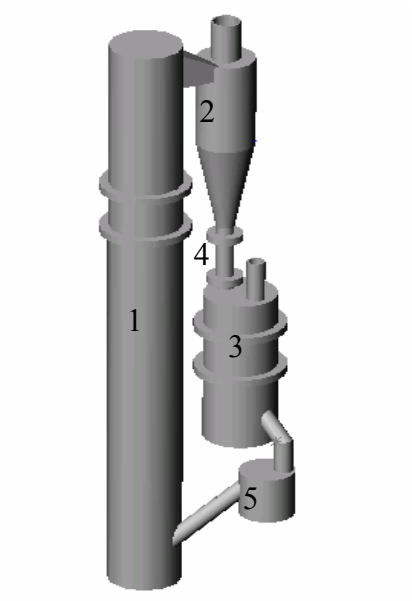

Figure 7. *Layout of the model. 1) air reactor, 2) cyclone, 3) fuel reactor, 4) downcomer 5) particle pot-seal*

Figure 8. *Picture of the experimental set-up*

Table 2 summarizes the scaling of a 30 MW_{th} CLC pressurized system to the ambient system. The basis for the scaling of the model is the air reactor, where the model has an inner diameter of 0.19 m and a height of 1.9 m, using air as fluid. The dimensions of the fuel reactor are also scaled, 0.19 m ID and 0.5 m in height, but since the fluid in the real combustor is a gaseous fuel, the density ratio in Equation (14) is not possible to fulfil with air. A hydrocarbon fuel would also react to form CO_2 and water, causing a dramatic increase in the volume flow as the gas passes the bed. This can obviously not be simulated in a cold model. For the circulation of particles the conditions in the air reactor are of most importance. The cyclone is not scaled, but was designed for optimal separation, and is therefore larger than the scaled size. The cold model is equipped with 24 pressure transducers. Most transducers measure differential pressure between two pressure taps, whereas a few measure the pressure difference from one tap to the atmospheric pressure. The taps are inclined at an angle of 45° to prevent blocking and they are connected to a three-way valve to facilitate purging.

Table 2. *Data for 30 MW_{th} unit and model scaled according to Equation (14)*

			30 MW_{th} unit	**Scaled model**
Fluid			air	air
Temperature	T	°C	1000	20
Pressure	p	Pa	$9 \cdot 10^5$	$1 \cdot 10^5$
Gas viscosity	μ	Pas	$48.8 \cdot 10^{-6}$	$1.81 \cdot 10^{-6}$
Gas density	ρ_g	kg/m^3	2.46	1.19
Bed geometry	L	m	L	L/10
Particle diameter	d_p	μm	300	150
Solids density	ρ_s	kg/m^3	5240	2600
Superficial velocity	u_0	m/s	u	$0.32 \cdot u$
Solids flux	G_s	kg/m^{2}s	G_s	$0.16 \cdot G_s$

The particles used are silica sand with a density of 2600 kg/m^3 and an average size of 0.15 mm. A small amount of Larostat® powder No 519 was added to lower the static electricity. The fluidizing gas was air, and all experiments were conducted at room temperature. The air is added in the bottom through perforated plates serving as air distributors, and the number and dimensions of the holes are calculated according to Kunii and Levenspiel (1991). The gas flows to the reactors are controlled by rotameters.

3.1.2 The cold-flow model of 300 W unit (Papers III-IV)

Most of the tests of oxygen-carriers have been carried out in batch type of reactors. Because of the high costs associated with producing large amount of oxygen-carrier particles there was a need for a continuously working chemical-looping combustion reactor of small size. The purpose of the reactor presented in papers III-IV is to design and build such a reactor system for tests of different oxygen-carriers in a continuous reactor. First a cold model was constructed and tested. Based on the results from the cold-flow model, a 300 W chemical-looping combustor was built and tested in actual operation (papers V-VI).

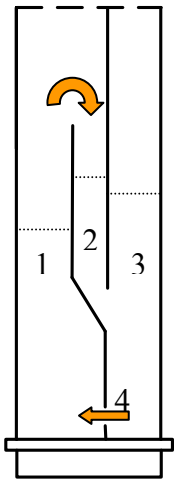

Figure 9. *A two-compartment fluidized bed. 1) air reactor, 2) downcomer, 3) fuel reactor, 4) slot*

The design of the two-compartment fluidized bed proposed by Chong (Chong et al. 1986) for oil shale retort is used in papers III-VI, see Figure 9. The air reactor, (1), has a higher velocity causing particles to be thrown upwards, and some of them fall into a downcomer, (2), leading to the fuel reactor, (3). There is a slot, (4), in the bottom of the wall between the two reactors, and the particles move through this slot from the fuel reactor to the air reactor.

The chemical-looping combustor was designed for a power range of 100 to 300 W depending on the fuel and the particle size and density of the oxygen-carrier. As basis for the design of the unit, was chosen particles with a density of 2300 kg/m^3 and a mean diameter of 95 μm. To simulate this, a suitable particle for the cold-flow model is powder used for fluid catalytic cracking (FCC), with a particle density of 1500 kg/m^3 and a mean particle diameter of 70 μm. The idealized relationships between the hot unit and the cold-flow model are shown in Table 3.

The dimensions of the system are very small and for this reason surface effects may not be negligible. The scaling rules are based on similarity in hydrodynamics and interparticle effects, whereas effects between particles and wall are neglected. This should be kept in mind when the results are transferred between the cold-flow model and the hot unit, but might not be crucial. The difference in size between the cold-flow model and the hot laboratory unit is quite small, although the hot unit is

somewhat bigger than the cold-flow model. Therefore the wall effects might be lesser in the hot unit, and the particle recirculation somewhat higher.

The pressure was measured along the height of the reactors. The gas flows were controlled by mass-flow controllers. A gas bubble meter was utilized to calibrate the mass-flow meters.

Table 3. *Idealized relationship between the hot laboratory unit and the cold-flow model.*

Parameter	Dimension	Chemical-looping combustor	cold-flow model
Gas, air reactor	-	air	N_2/He (13/87)
Gas, fuel reactor	-	CO/H_2 (50/50)	N_2/He (13/87)
Temperature	T	950°C	25°C
Particles		oxygen-carrier	FCC
Mean diameter	μm	95	70
Density of particles	kg/m^3	2300	1500
Length	m	L	0.75*L
Area	m^2	A	0.56*A
Superficial velocity	m/s	u	0.86*u
Volume flow	m^3/s	U	0.48*U
Circulation rate	kg/s	M_{circ}	0.74*M_{circ}

The cold-flow model, Figure 10, has some fixed dimensions and some which could be slightly varied. The cross-section of the fuel reactor is constant with both a depth and width of 19 mm. The air reactor had a larger cross-sectional area in the bottom, see Figure 9, where the dimensions were 19×27 mm. In the top section next to the downcomer, the area was smaller with a width of either 15 of 17 mm. Further, the height from the bottom plate to the slot is 4 mm, the height from the bottom plate to the downcomer exit 38 mm, and the total height of the downcomer, including the sloped part, is 85 mm. The height of the slot between the reactors was varied between 1.2 and 8 mm. The profile of the wall beneath the slot was altered from the shape of

an I to a T by adding a horizontal plate beneath the slot. The width of the downcomer was also altered between 9 and 11 mm. The different designs are presented in Table 4.

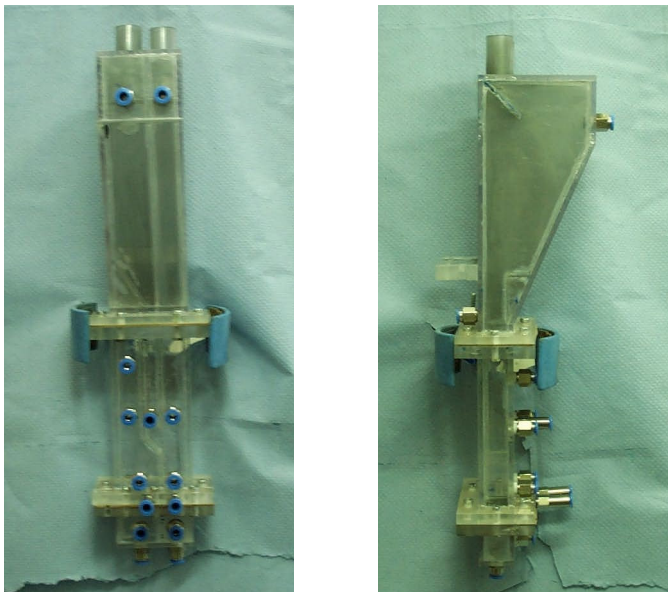

a) frontview b) sideview

Figure 10. *The cold-flow model.*

Table 4. *Design variations and main dimensions*

design	FR dimension	AR dimension (bottom)	Downcomer width	Slot height	Slot profile
	[mm]	[mm]	[mm]	[mm]	[mm]
A	19 × 19	19 × 27	9	8	I
B	19 × 19	19 × 27	9	4.5	I
C	19 × 19	19 × 27	11	1.5	I
D	19 × 19	19 × 27	11	1.2	T

3.1.3 The 300 W unit (Papers V-VI)

With the experience gained in the work with the cold-flow model presented in papers III and IV, a 300 W chemical-looping combustor was constructed and is presented in papers V-VI. The design is the same as the cold-flow model in papers III and IV, but with some minor changes. A possibility to fluidize the downcomer is added, and the slot is somewhat altered with fluidization possibilities, see Figure 11.

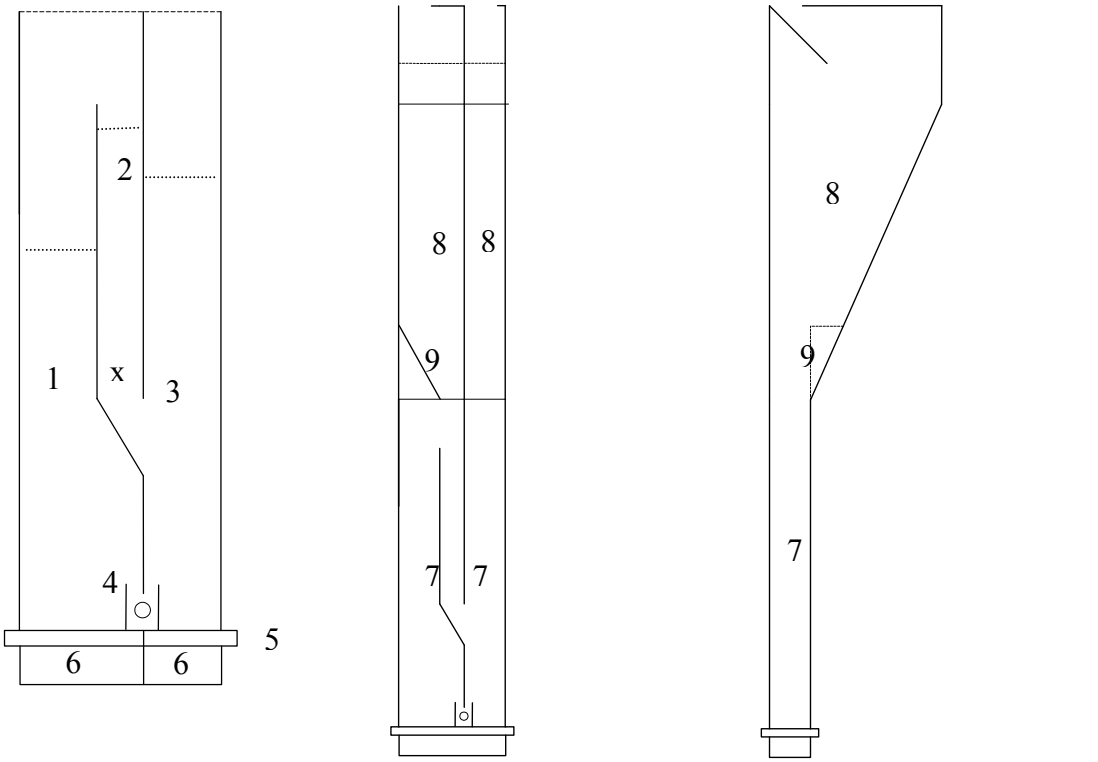

a) the lower part, frontview b) entire reactor, frontview c) entire reactor, sideview

Figure 11. *The principal sketch of the reactor. 1) air reactor, 2) downcomer, 3) fuel reactor, 4) slot, 5) gas distributor plate, 6) wind box, 7) reactor part, 8) particle separator, 9) leaning wall. Fluidization in the downcomer (x) and slot (o) is also indicated. The dashed lines in 2a indicate typically expected bed heights during combustion.*

The reactor is designed to work with a thermal power in the range 100 to 300 W for either natural gas or syngas as fuel. Depending on size and density of the oxygen-carrier particles, the thermal power might have other limits.

The experimental set-up is shown in Figure 11 and Figure 12. The air reactor, (1), has a velocity high enough for particles to be thrown upwards, with a certain fraction of them falling into a downcomer, (2), leading to the fuel reactor, (3). There is a particle column in the downcomer preventing gas to leak between the reactors. Particles that fall into the downcomer increase the column height and create a pressure, forcing particles into the fuel reactor. Thereby, the bed height and pressure are also increased in the fuel reactor. The higher pressure in the fuel reactor forces the particles through the opening (4), situated in the bottom of the wall between the reactors, back into the air reactor.

Figure 12. *The hot chemical-looping combustor*

Fuel and air enter in two separate wind boxes, and two porous quartz plates act as distributors for the gases entering the reactors. The fuel reactor has a depth and a width of 25 mm. The dimensions of the air reactor are 25×40 mm in the bottom, and 25×25 mm in the upper narrow part. The reactor part is 200 mm high, and above this part a section for separation of particles is situated. In this section the reactors widen to decrease the gas velocities and allow particles to fall back into the reactors, Figure 11c. The particle separation section is totally 240 mm high, in the first 180 mm the reactor depth expands from 25 mm to 105 mm. The last 60 mm has a constant cross-section area, and just before the exits of the reactors a leaning plate is added to reduce elutriation of particles. The particles falling down in the sloping section above the air reactor are led to the downcomer by a leaning wall, Figure 11b-c. The downcomer has a width of 12 mm and the upper part of the wall separating it from the air reactor ends at 170 mm height. The upper part of the downcomer opening to the fuel reactor is at a height of 75 mm and this opening is 25 mm high. It is possible to add a gas in the side of the downcomer, and in that way fluidize the particle column. Tests in the cold-flow model show that this improves particle circulation. The slot in Figure 11 through which the particles from the fuel reactor are circulated to the air reactor was designed to minimize gas leakage between the reactors. It has two 15-mm walls rising from the

bottom plate, separated by 10 mm. The single wall separating the fuel and air reactor is situated between these two walls and stops 11 mm above the bottom plate, Figure 11a. Between the two walls is a pipe, and this pipe has three 1-mm holes directed downwards through which fluidizing gas, e.g. argon, is injected.

The two gas flows leaving the reactors are each connected to a gas sampling system containing particle filter, cooling system for condensation of water and on-line gas analysers (SICK MAIHAK S710). The following gases are possible to measure with the analysers: carbon monoxide, carbon dioxide, oxygen and methane. Measurements of H_2, CO and CO_2 in the gas stream from the fuel reactor were also made with a gas chromatograph (Varian Micro-GC CP4900 equipped with a Molesieve 5A and PoraPLOT Q column). On the exit pipe from the fuel reactor, there is a water trap. The height of the water column can be varied and thus the water trap can be used to control the pressure balance between the reactors.

3.2 Experimental procedure

3.2.1 Circulation flow of particles in a CFB-like model (Paper I)

The model shown in Figure 7 and Figure 8 was operated with different solids inventories in the range from 5 to 10 kg. The superficial gas velocity in the air reactor (riser) was varied from 0.7 to 1.2 m/s, while the velocity in the fuel reactor was held constant at 0.12 m/s in all runs. The latter corresponds to a flow that is somewhat lower than the product gas flow of CO_2 and H_2O.

The net solids flux, G_s, was measured by closing a butterfly valve situated in the downcomer after the cyclone. Pressure drop in the reactors was measured to obtain the solids hold-up and the vertical distribution of solids in the riser.

3.2.2 Gas leakage between two reactors in a CFB-like model (Paper II)

The model was operated with 9 kg of sand. The velocity in the air reactor was varied between 0.75 and 1.15 m/s, the velocity in the fuel reactor from 0.09 to 0.31 m/s, and the velocity in the particle lock between 0.065 and 0.097 m/s. Helium was added to

the inlet air in one of the following: fuel reactor, air reactor or particle pot-seal. The concentration of helium was measured with a mass spectrometer either in the outgoing gas flows from the cyclone, the fuel reactor, or in the outlet from the particle pot-seal into the air reactor. The leakage is defined as the fraction of gas added to one reactor, which escapes out of the other reactor.

3.2.3 Circulation flow and gas leakage in a cold-flow model of a 300 W unit (Papers III-IV)

The cold-flow model was operated with FCC particles, and the total solids inventory was varied between 40 and 70 g. The gas volume flow in the air reactor varied from 5 to 7 L/min. This gives a velocity in the narrow part of the riser of 0.26 to 0.36 m/s for deigns A and B, and a velocity of 0.29 to 0.41 m/s for designs C and D. The reason for the different gas velocities is due to the change in downcomer width, causing a change in the riser cross-sectional area. The different designs are presented in Table 4. The gas flow in the fuel reactor was varied between 1.1 and 3 l/min giving the velocities of 0.05 to 0.14 m/s. In addition to variations of the slot design and gas velocities the additional fluidisation of the downcomer was tested.

A very simple tracer method was used to determine the solids circulation rate. As the bed material was white, a very fine black powder (ground coal dust) was introduced in the downcomer at the top surface of the particle column. The time for the tracer "point" to move a certain distance was measured, giving the velocity of the particle column. For confirmation of the results, a second measurement method was used. A small ball was introduced in the downcomer, and was taken along by the moving solid column. The movement of a thin thread connected to the ball indicated the velocity of the moving solids column and therefore also the mass flow.

For gas leakage measurements the nitrogen in the standard fluidization gas in one of the reactors was substituted with air, which results in an oxygen concentration of 2.73%vol. The oxygen concentration out from both reactors was measured. Also the outlet volume flows and concentration of the inlet air/helium gas were measured to verify the quality of the results.

3.2.4 Leakage and combustion measurements in a 300 W unit (Paper V)

Leakage tests as well as combustion tests with natural gas, consisting of 88% methane and with an H/C ratio of 3.7, were performed in the reactor shown in Figure 12. The leakage tests were made to assess the performance of the reactor system and to support the evaluation of data from the combustion tests.

The oxygen-carrier used has nickel oxide as active part, and magnesium aluminates as support material, $NiO/MgAl_2O_3$. The mass fraction of active/support material in the particle is 60/40%. The total solids inventory used was 340 g.

The first leakage test series was made with carbon dioxide as fluidization gas in the fuel reactor, air in the air reactor and argon in the downcomer and the slot. The volume percentage of carbon dioxide and oxygen was measured in both outgoing gas streams. In all leakage tests the temperature in the fuel reactor was 850°C. Table 5 shows the volume flows in the different tests.

The second series of leakage measurements was made with carbon dioxide instead of argon in the downcomer and slot, nitrogen in the fuel reactor and air in the air reactor. The same tests were made as for the first leakage series.

Table 5. *First and second leakage test series.*

Test number	U_{FR} L_n/min	U_{AR} L_n/min	U_{DC} L_n/min	U_{SL} L_n/min	T_{FR} °C
L1	0.15-0.9	6	0.01	0.02	850
L2	0.35	4-6.5	0.01	0.02	850
L3	0.15-0.55	1.7-6.3	0.01	0.02	850
L4	0.35	4	0-0.04	0.02	850
L5	0.35	4	0.01	0.01-0.04	850

L_n is the flow normalised to 0˚C and 1 bar.

Combustion measurements with natural gas as fuel in the fuel reactor were also made. The fuel flow, the air flow and the temperature in the reactors were varied one at a time, see Table 6.

Table 6. *Combustion test series with natural gas as fuel.*

Test number	U_{FR} L_n/min	U_{AR} L_n/min	U_{DC} L_n/min	U_{SL} L_n/min	T_{FR} °C
N1	0.15-0.55	6	0.01	0.02	850
N2	0.35	4-6.5	0.01	0.02	850
N3	0.35	4	0.01	0.02	800-950

3.2.5 Combustion measurements in a 300 W unit (Paper VI)

In this paper the oxygen-carrier described above was used, but also another oxygen-carrier was tested with combustion. This oxygen-carrier was also based on nickel oxide and alumina. The particle was developed in the EU financed GRACE project, and has been previously used in testing in a 10 kW chemical-looping combustor (Lyngfelt and Thunman 2005) The total solids inventory was 340 g for both particles.

Two combustion test series were performed, one with natural gas as fuel, and one with a mixture of 50% CO and 50% H_2 as fuel. The natural gas consists of 88% methane, and has a H/C ratio of 3.7, and the mixture of CO and H_2 has a concentration ratio of 50/50. The GRACE particle was tested with natural gas, and the results were compared with the results from the combustion tests made in Paper V. The $NiO/MgAl_2O_4$ particles were tested with syngas. The fuel flow, the air flow and the temperature in the reactors was varied one at a time. The test parameters for natural gas and syngas are shown in Table 6 and Table 7 respectively.

Table 7. *Combustion test series with syngas as fuel.*

Test number	U_{FR} L_n/min	U_{AR} L_n/min	U_{DC} L_n/min	U_{SL} L_n/min	T_{FR} °C
S4	0.5-1.3	6	0.01	0.02	850
S5	0.9	3.5-6.0	0.01	0.02	850
S6	0.5-1.3	2.5-6.5	0.01	0.02	850
S7	0.35	4	0.01	0.02	800-950

Measurements of concentrations of CO, CO_2, CH_4 and O_2 in the streams leaving both reactors were made using on-line gas analysers (SICK MAIHAK S710). When syngas was used as fuel, measurements of H_2, CO and CO_2 in the gas stream from the fuel reactor were also made with a gas chromatograph (Varian Micro-GC CP4900 equipped with a Molesieve 5A and PoraPLOT Q column).

4 RESULTS AND DISCUSSION

Experimental studies of reactor systems for chemical-looping combustion have been performed. One purpose of this work was to evaluate the suitability of different designs as possible choices as full-scale plants and laboratory reactors. An additional goal was to demonstrate this new combustion technology in a small scale and test the performance of oxygen-carrier particles in real operation. This thesis presents data from two types of cold-flow units and one 300 W chemical-looping combustor.

The first, a CFB-like design, was proposed as a design possibility for a 30 MW pressurized chemical-looping combustor. It was built as a cold-flow model in Perspex, and circulation of particles (Paper I) and leakage of gas between the reactors (Paper II) were measured.

The second type of reactor system was designed primarily for testing smaller amounts of oxygen-carriers in real operation. A simpler design than the CFB-like reactor tested above was preferred, and a two-chamber fluidized bed was chosen. In order to evaluate its suitability as a chemical-looping combustor, this simpler design was first built as a cold-flow model, and tested with respect to particle circulation and gas leakage (Papers III and IV). Thereafter a hot unit was built and operated with two different nickel-based oxygen-carriers (Papers V and VI). Leakage and combustion tests with natural gas and syngas were investigated.

Below, some major quantitative results are given. The full results can be found in the enclosed papers.

4.1 The CFB-like model (Papers I-II)

4.1.1 Solids circulation

The rate of circulation of solid material from the air to the fuel reactor, i.e. the net solids flux, G_s, is dependent on both the fluidization velocity and the total mass of bed material in the system, Figure 13. Figure 14 shows the net solids flux as a function of the superficial velocity for different total pressure drops over the air reactor. As can be seen in Figure 14 it is clear that G_s is rather independent of the pressure drop of the riser in the range 0.6 to 1.2 kPa. This indicates that the circulation of particles is almost independent of the bed mass when there is enough bed material in the system to give a pressure drop of at least 0.6 kPa in the riser. In this system, the fuel reactor and the pot-seal will first be filled to their overflows, the rest of the particles will be in the air reactor and circulation system. Figure 13 indicates that 5 and 6 kg is not enough for this system since the air reactor will be emptied, and thus the solid flux will be lost.

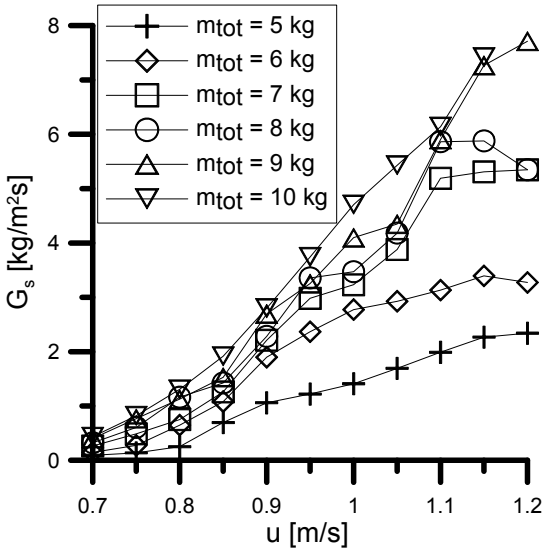

Figure 13. *Average values of G_s versus superficial velocity in the air reactor.*

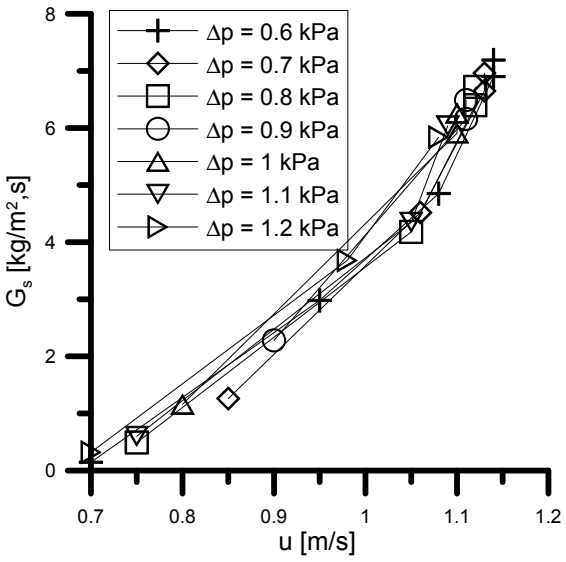

Figure 14. *G_s versus velocity for different pressure drops*

The highest measured net solids flux in the cold model corresponds to a scaled up solids flux of 48 kg/m^{2}s, or 4.6 kg/s,MW$_{th}$. The limit of the solids flux was caused by the return system, i.e. the particle flow coming out of the downcomers. Concerning oxygen transport, the mass flow measured is most likely sufficient for metal oxides

like nickel oxide, copper oxide and manganese oxide, but there is an uncertainty whether a flow of 4.6 kg/s,MW_{th} would be sufficient for iron oxide, Fe_2O_3. If a solids circulation of 4 kg/s,MW_{th} is to be enough the change in mass conversion, $\Delta\omega$, over a cycle has to be 0.02. This corresponds to a complete conversion of Fe_2O_3 to Fe_3O_4 if there is 40% inert material in the particle, (Mattisson et al. 2004). Because of thermodynamic restraints it is not possible to use lower forms of iron oxide, i.e. FeO, (Mattisson and Lyngfelt 2001). Thus, iron oxide might require a somewhat higher fluidization velocity compared to those used in the present study to reach a sufficient recirculation.

4.1.2 Gas leakage

Under normal operating conditions the gas leakage between the fuel and air reactor is small. The pressure balance for the system is important for the gas leakage. The pressure difference between the fuel reactor and the rest of the system should be as small as possible. If the fuel reactor pressure deviated much from the rest of the system large leakages occurred. The pressure in the fuel reactor should be higher than in the cyclone, but lower than in the air reactor and the particle pot-seal.

The gas leakage from the fuel reactor to the air reactor depends on the velocity in the fuel reactor, see Figure 15. At normal operating conditions, the leakage is about 2%, which means that 2% of the carbon dioxide will not be captured. This gas leakage is reduced as the net solids flux is increased. At high net solids flux as the particles in the downcomer will not be fluidized but instead the particles will entrain gas from the cyclone down into the fuel reactor.

The leakage from the particle pot-seal to the fuel reactor depends on the velocity in the pot-seal, see Figure 16. The total range of leakage from the pot-seal to the fuel reactor was 2-12%, which, if fluidized by air, would cause a dilution of the produced CO_2 by 2.4 to 15% air. This leakage is probably high enough to motivate countermeasures, for instance fluidization with steam instead of air below the downcomer.

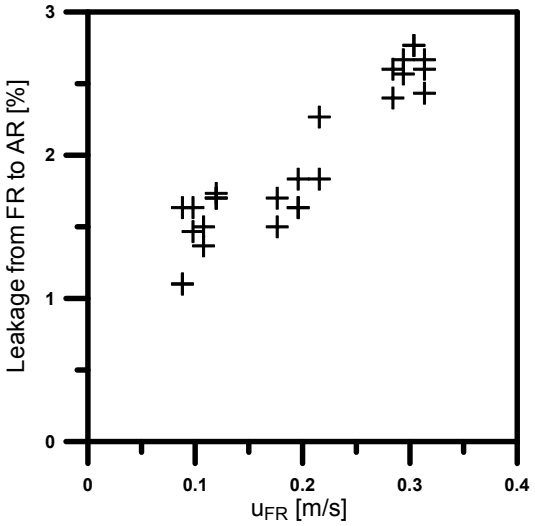

Figure 15. *Leakage from the fuel reactor to the cyclone, against the velocity in the fuel reactor, u_{FR}*

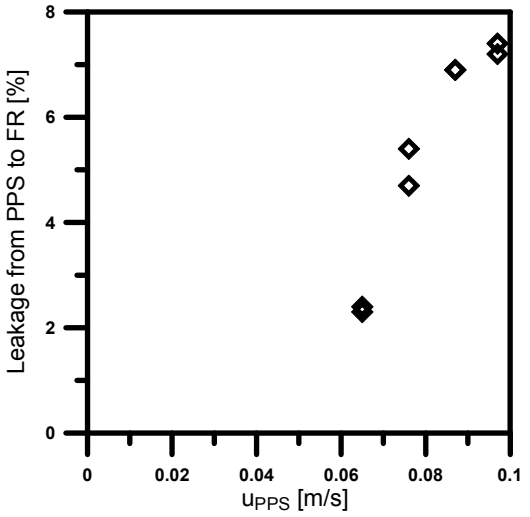

Figure 16. *Leakage from the particle pot-seal (pps) to the fuel reactor, against the velocity in the particle pot-seal, u_{PPS}*

Helium was added in the air reactor, and the concentration out from the fuel reactor measured. This was made to investigate whether the carbon dioxide would be diluted by nitrogen or not. No leakage in this direction could be detected.

4.2 The cold-flow model of a 300 W unit (Papers III-IV)

4.2.1 Solids circulation

Figure 17 shows the solids circulation rate against the velocity in the air reactor, for the four different designs, see Table 4. By velocity in air reactor is meant the velocity in the upper, narrow part, along the downcomer. Since two of the designs, C and D, have a more narrow section, they will have higher velocities for the three volume flows used. The velocity in the fuel reactor is held constant at 0.05 m/s, which corresponds to 100 W in the hot laboratory unit. The trend is that the lower the slot height, the lower is the particle flow between the reactors. However, the design with the largest slot, A, did not have the highest recirculation.

The needed solids circulation is expected to fall within the range 2-8 g/s,kW depending on the metal oxide used, the inert fraction and the conversion in each cycle. Typically CuO and NiO needs lower solids circulation, and Fe_2O_3 the highest. For a particle with a needed solids circulation of 2 g/s,kW in the hot unit, this would

correspond to 0.15 to 0.44 g/s in the cold unit for 100 to 300 W respectively. These solids circulation rates are fulfilled, see Figure 17 and Figure 18. For a particle which has less oxygen available for reaction and thus with a higher solid circulation demand, rates of up to 8 g/s,kW may be needed. This would correspond to 0.6 to 1.8 g/s in the cold unit for 100 and 300 W. Thus it should be possible to run the hot unit with a 100 W load.

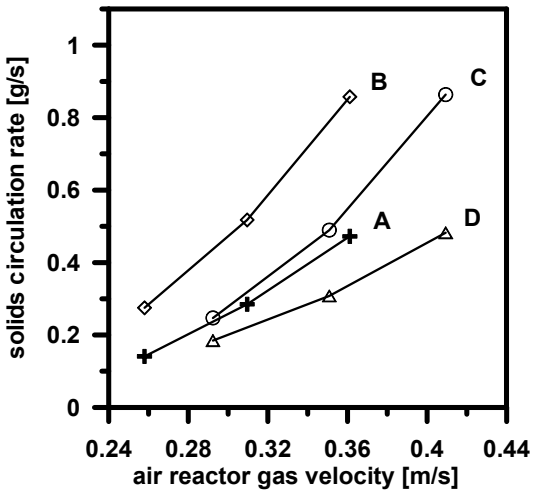

Figure 17. *Solids circulation rate for all designs and FCC powder. U_{FR}=0.05 m/s, total solids inventory=53 g.*

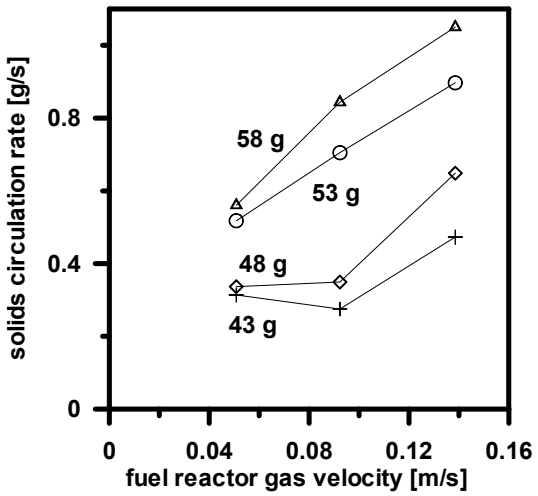

Figure 18. *Solids circulation rate for design B and different total solids inventory vs. u_{FR}. u_{AR}= 0.31 m/s, FCC powder.*

The influence on the velocity in the fuel reactor on the solids circulation flow is shown in Figure 18. As can be seen the circulation flow increases somewhat with increased velocity. Most likely the explanation to this is the more vigorous fluidization.

4.2.2 Gas leakage

In general it was found that gas leakage is directly related to the cross section of the slot opening. It is likely that the main mechanism of leakage is the exchange of gas bubbles reaching accidentally the other reactor through the opening. This is also suggested by the observation that there is a simultaneous leakage in both directions. Design D gives a lower gas leakage. The horizontal plate reduces this gas exchange

and also visual observations support the assumption that fewer gas bubbles cross the orifice and get into the other reactor.

Leakages occur both from the fuel reactor to the air reactor, and from the air reactor to the fuel reactor, see Table 8. Generally, the leakages between the two reactors are in the same order of magnitude. The difference is within a factor of two in almost all cases. The problem with leakage from the fuel reactor is a loss of carbon dioxide. The leakage in the other direction dilutes the exhaust gas from the fuel reactor. Therefore both leakage flows are suitable to relate to the incoming flow in the fuel reactor, i.e. the last column in Table 8.

Table 8. *Comparison of leakage flows. Design C and D,* u_{FR} *= 0.05 m/s,* u_{AR} *= 0.35* m/s

		Leakage flow, l/min	Fraction of air flow	Fraction of fuel flow
Design C	Leakage into FR	0.21	3.6%	19.5%
	Leakage into AR	0.13	2.1%	11.7%
Design D	Leakage into FR	0.037	0.6%	3.3%
	Leakage into AR	0.069	1.2%	6.3%

4.3 The 300 W unit (Papers V-VI)

4.3.1 Gas leakage

After construction of the 300 W chemical-looping combustor, a series of leakage tests were conducted, see Table 5. Leakages occur both from the fuel reactor to the air reactor, and from the air reactor to the fuel reactor. As mentioned above, the problem with leakage from the fuel reactor is a loss of carbon dioxide. This loss is here called leakage and is related to incoming flow in the fuel reactor, thus indicating the percentage of carbon which is lost to the air reactor. The leakage in the other direction dilutes the exhaust gas in the fuel reactor. Therefore also this leakage is suitable to relate to the incoming fuel flow, and is referred to below as dilution. Thus the leakage, L, and dilution, D, are defined as:

$$L = \dot{n}_L / \dot{n}_F \tag{15}$$

$$D = \dot{n}_D / \dot{n}_F \quad (16)$$

where $\dot{n}_L$ is the molar flow of gas leaking from the fuel to the air reactor, $\dot{n}_F$ is the molar flow of gas entering the fuel reactor and $\dot{n}_D$ is the molar flow of gas leaking from the air to the fuel reactor.

The leakage and the dilution are shown in Figure 19 as a function of the flow rate to the fuel reactor. Both the leakage and dilution are highly dependent on the fuel flow and the leakage varies from 35 to 15% while the dilution varies from 25 to 10%. A higher flow in the fuel reactor significantly decreases both the leakage and dilution. However, the absolute leakage flows in both directions, $\dot{n}_D$ and $\dot{n}_L$ increase. The two beds are connected via the slot. Pressure fluctuations and passing bubbles cause gas exchange in both directions. A higher fuel flow leads to more vigorous fluidization, which may result in higher flows from the fuel reactor to the air reactor. All the same, the leakage and dilution, which are related to the fuel flow, $\dot{n}_F$, decrease as the fuel flow increase. The leakage from the fuel reactor is roughly twice as large as the dilution of the fuel reactor, which is also seen in the tests reported below. A reason for the higher leakage to the air reactor compared to leakage in the opposite direction is believed to be the higher pressure in the fuel reactor compared to the air reactor. The downcomer is also preventing gas to leak from the air reactor to the fuel reactor, while some gas from the fuel reactor may pass the column upwards.

The leakage and dilution measured in combustion test N1 are also shown in Figure 19. These measurements are more scattered, but gave a similar decreasing trend of the leakage, and in the same range, as the leakage tests. The leakage in the combustion tests is measured directly as the amount of carbon dioxide out from the air reactor, the dilution from the same tests is measured indirectly as the total flow out from the fuel reactor minus the flow of CO, CO_2, CH_4 and inert gas, and therefore the uncertainty is higher. Leakage and dilution measured in combustion tests are not directly comparable with the leakage and dilution tests without combustion, since there is a gas flow reduction in the air reactor due to oxygen reacting with the oxygen-carrier and a gas flow increase in the fuel reactor due to formation of CO_2 and H_2O from the fuel. The reduction in the air reactor is not very high because of the excess of air, but the reactions in the fuel reactor cause a significant flow increase.

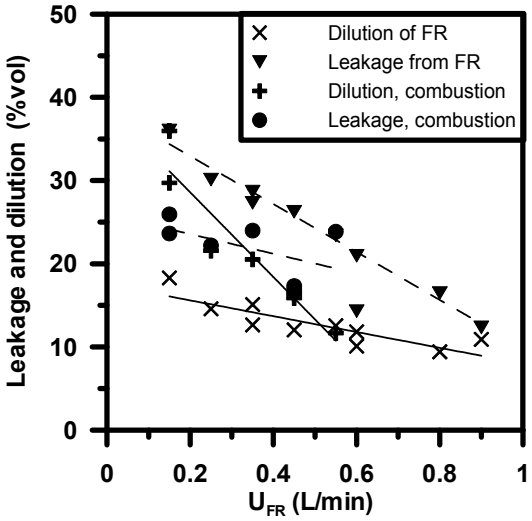

Figure 19. *The leakage and dilution as a function of the volume flow in the fuel reactor, U_{FR}. Test L1 and leakage from test N1.*

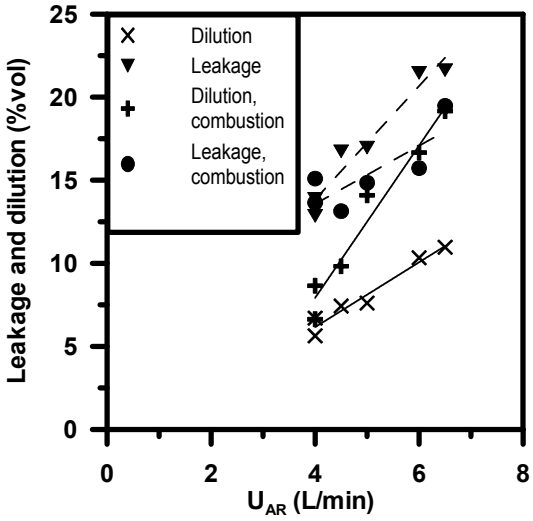

Figure 20. *The leakage and dilution as a function of the volume flow in the air reactor, U_{AR}. Test L2 and leakage from test N2.*

The leakage from the fuel reactor increases as the velocity in the air reactor increases, Figure 20. Several mechanisms could explain this. Firstly, a higher particle circulation causes a higher pressure in the fuel reactor. Secondly, some gas is expected to follow the particles, and therefore would a higher particle circulation cause higher leakage. Thirdly, an increase of pressure fluctuations should promote the gas exchange through the slot. The latter could also explain why the leakage into the fuel reactor, i.e. the dilution, increases as the velocity in the air reactor increases. The leakage and the dilution vary in the range 13-22% and 5-10%. This is lower than in the previous test series shown in Figure 19, which was made at a high air flow. The leakage and dilution measured in combustion test N2 are also shown in the figure. Again the leakage and dilution were of the same order as in the leakage tests, and also the trends were the same.

4.3.2 Combustion

The carbon monoxide in the gas from the fuel reactor is presented below as fraction of total carbon leaving the fuel reactor, i.e. CO, CO_2 and CH_4.

$$f_{CO} = \frac{x_{CO}}{x_{CO_2} + x_{CO} + x_{CH_4}} \tag{17}$$

where x_i is the molar fraction of i in dry exit gas from the fuel reactor. Similarly, the methane and hydrogen in the flue gas is given as fraction of total carbon.

$$f_{CH_4} = \frac{x_{CH_4}}{x_{CO_2} + x_{CO} + x_{CH_4}} \tag{18}$$

$$f_{H_2} = \frac{x_{H_2}}{x_{CO_2} + x_{CO} + x_{CH_4}} \tag{19}$$

The actual concentrations of CO, CH_4 and H_2 are somewhat lower because of the dilution by nitrogen from the air reactor and inert gas from the downcomer and slot. The conversion of natural gas to carbon dioxide is high for both of the tested Ni based particles for all the investigated conditions. For the GRACE particle the fraction of CO is rather constant around 0.5%, i.e. very close to thermodynamic equilibrium at 850°C. For this carrier there was always some CH_4 from the outlet of the fuel reactor, typically 0.5-1.5%. Unconverted methane has been found in previous work with this particle in tests with high circulation (Lyngfelt and Thunman 2005), and was associated with high degree of oxidation of the particle which inhibits intermediate reforming steps which occur on nickel surface. The other particle, $NiO/MgAl_2O_4$, converts all the methane, but gives a higher amount of carbon monoxide than the equilibrium, typically 0.5-3%. Thermodynamic calculations show that NiO can not convert methane to CO_2 and H_2O completely, but at equilibrium conditions some CO and H_2 will be present. At 850°C the fraction of CO, f_{CO}, is 0.71% at equilibrium and the fraction of H_2 of the total hydrogen, i.e. $f'_{H_2} = x_{wet,H_2} / \left(x_{wet,H_2} + x_{wet,H_2O}\right)$ is 0.64% at equilibrium. The value of f_{H_2}, see eq (19), at equilibrium is dependent on the hydrogen to carbon ratio of the fuel, which is 3.7 for natural gas. Thus, f_{H_2} at equilibrium is $f'_{H_2} \cdot 3.7/2 = 1.17$.

For the experiments conducted with syngas and the $NiO/MgAl_2O_4$ oxygen-carrier, the carbon monoxide is presented below as f_{CO}, the fraction of carbon products leaving the fuel reactor,

$$f_{CO} = \frac{x_{CO}}{x_{CO_2} + x_{CO}} \tag{20}$$

and the hydrogen is presented in a similar way, i.e. as the fraction of total hydrogen leaving the reactor, f_{H_2}. Since the fuel consists of 50% CO and 50% H_2, the total molar amount of H_2 plus H_2O leaving the reactor is equal to CO plus CO_2.

$$f_{H_2} = \frac{x_{wet,H_2}}{x_{wet,H_2O} + x_{wet,H_2}} = \frac{x_{dry,H_2}}{x_{dry,CO_2} + x_{dry,CO}} \tag{21}$$

The degree of unburnt increases as the fuel load increases, see Figure 21 and Figure 22. This is expected, firstly because a larger amount of fuel has to react with the same amount of particles. Secondly, there is also a less efficient contact between the particles and the gas at higher velocities when a larger fraction of the gas will be in the bubble-phase.

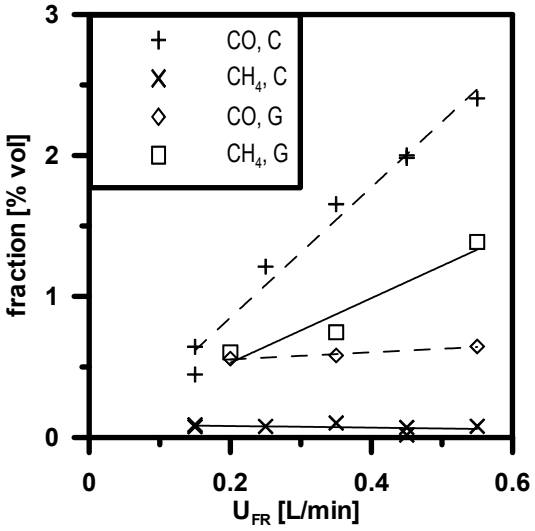

Figure 21. *Fraction of carbon monoxide (dashed lines) and methane (continuous lines) in the combustion products, as a function of the flow in the fuel reactor. C is the CCCC particle NiO/MgAl2O4, and G is the GRACE particle. Results with natural gas, test series N1.*

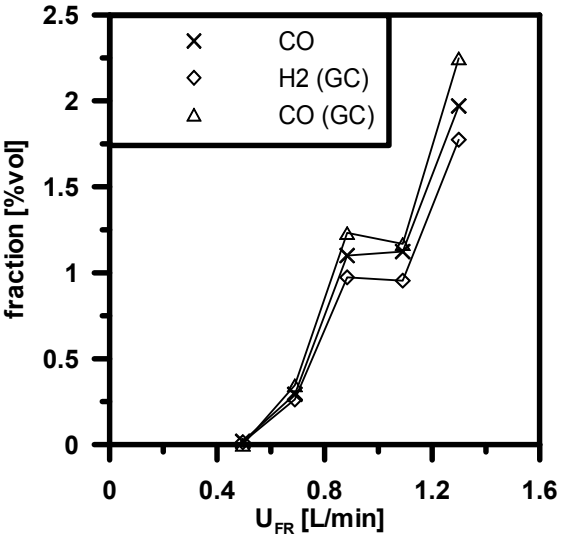

Figure 22. *Fraction of carbon monoxide and hydrogen in the combustion products, as a function of the flow in the fuel reactor. Result with syngas, test series S1.*

For natural gas, a slight decrease of the CO fraction for the $NiO/MgAl_2O_4$ particle can be seen when the velocity in the air reactor increases, see Figure 23. For the GRACE particle, the CO is approximately constant and CH_4 increases somewhat. When syngas is used as fuel, an increase of the gas flow in the air reactor decreases the

concentration of carbon monoxide and hydrogen in the flue gas from the fuel reactor, Figure 24. An increased air flow means a higher concentration of oxygen in the air reactor and also a higher circulation rate of the particles, which was shown in Papers III and IV. The decrease is small though, and could also be an effect of increased leakage.

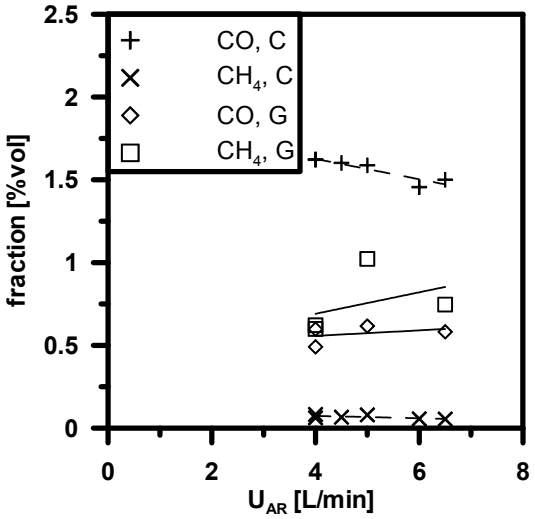

Figure 23. *Fraction of carbon monoxide (dashed lines) and methane (continuous lines) in the combustion products, as a function of the flow in the air reactor. C is the CCCC particle NiO/$MgAl_2O_4$, and G is the GRACE particle. Results with natural gas, test series N2.*

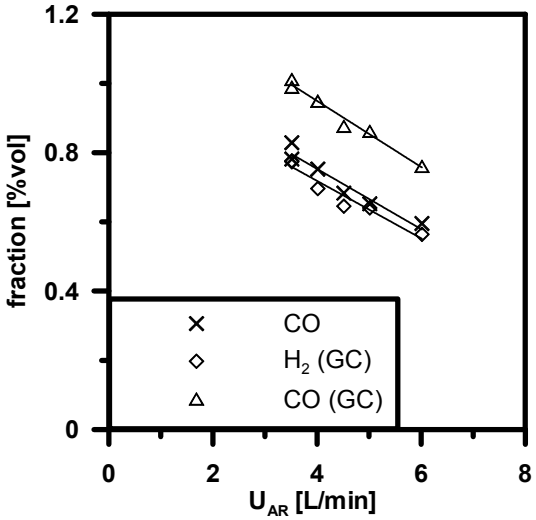

Figure 24. *Concentration of carbon monoxide and hydrogen in the combustion products, as a function of the flow in the air reactor. Results with syngas, test series S2.*

The gas conversion for both oxygen-carriers with natural gas is shown as a function of temperature in Figure 25. The fractions of methane and carbon monoxide for the GRACE particle were both about 0.5% in the temperature range tested. For the other particle, NiO/$MgAl_2O_4$, methane was close to zero while CO was about 3% at 800°C, but this fell to 1.5% at the higher temperatures tested. The equilibrium line for CO in the flue gas is also shown in Figure 25. This shows that the GRACE particle gives a fraction of CO that fits well with the equilibrium, while the NiO/$MgAl_2O_4$ particle does not reach equilibrium for carbon monoxide. However, from the figure it seems as if the fraction of CO approaches equilibrium at the higher temperatures. To be noted is that the reactivity of the two particles is reversed for methane compared to CO, i.e. the methane fraction is close to the equilibrium which is 0% for the NiO/$MgAl_2O_4$ particle and significantly higher for the GRACE particle.

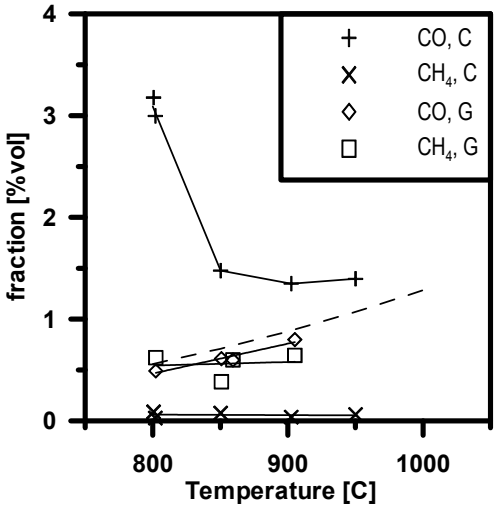

Figure 25. *Fraction of carbon monoxide and methane in the combustion products, as a function of the temperature in the fuel reactor. Results from test series N3. C is the CCCC particle NiO/MgAl$_2$O$_4$, and G is the GRACE particle. The dashed line is the equilibrium line for CO.*

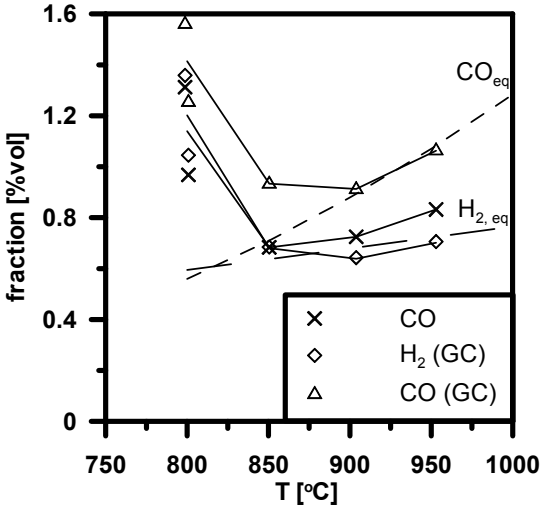

Figure 26. *Fraction of carbon monoxide and hydrogen in the combustion products, as a function of the temperature in the fuel reactor. Results from test series S4. The dashed lines are the equilibrium lines for CO (short lines) and H_2 (long lines).*

With syngas the degree of conversion to CO_2 is also improved at higher temperatures for the CCCC particle, as is seen in Figure 26. From 900°C the CO and H_2 reach and follow the equilibrium lines, and thereby the conversion decreases. However, even at a low temperature of 800°C the conversion of syngas to carbon dioxide and water is high. The equilibrium lines for carbon monoxide and hydrogen are also presented in the figure. At temperatures from 850°C the fraction of hydrogen reaches equilibrium. Measured with the gas chromatograph (GC), carbon monoxide reaches equilibrium at 900 and 950°C, but the measurements with the gas analyser show a somewhat lower fraction of carbon monoxide than equilibrium.

A possible explanation for fractions lower than equilibrium seen in Figure 26 and especially in Figure 22 is that some of the oxygen leaking from the air to the fuel reactor does not react on the way up through the bed, but reacts with carbon monoxide and hydrogen above the bed, thus lowering the concentrations below the equilibrium values. Normally, the leakage of oxygen is in the order of 1% of the total oxygen supplied to the fuel in the fuel reactor and since most of this oxygen is likely to be consumed in the lower part by reaction with particles or fuel, the leakage is expected

to have a minor effect on the outgoing concentrations. However, during conditions with a low flow in the fuel reactor and a high flow in the air reactor, the leakage of oxygen from the air reactor to the fuel reactor is larger, up to 6% of the total oxygen supplied to the fuel in the fuel reactor. Thus, a possible explanation for these low fractions is that some of the oxygen leaking from the air reactor does not react on the way up through the bed, but reacts with carbon monoxide and hydrogen above the bed, thus lowering the concentrations below the equilibrium values.

Table 9 gives a summary of gas fraction out of the fuel reactor, and combustion efficiency compared to the theoretical maximum combustion efficiency. The results presented are from tests N3 and S4 at 850°C. For syngas results are shown both for online gas analyser (GA) and for gas chromatograph (GC). The combustion efficiencies are all close to the theoretical maximum. The fraction of hydrogen for natural gas and the $NiO/MgAl_2O_4$ particle was not measured but assumed based on the water shift equilibrium. It is possible that this value is overestimated, causing a lower combustion efficiency. The value of the combustion efficiency is probably lower than the efficiency for the GRACE particle, but the amount is uncertain.

Table 9. *Summary of gas fractions out from the fuel reactor, and combustion efficiencies.*

	f_{H_2} [%]	f_{CO} [%]	f_{CH_4} [%]	$\eta_{combustion}$ [%]	$\eta_{theoretical\ maximum}$ [%]
Natural gas, G	1.17[1]	0.71[1]	0.38	98.98	99.42
Natural gas, C	3.03[2]	1.48	0.08	98.40	99.42
Syngas, C (GC)	0.68	0.94		99.18	99.32
Syngas, C (GA)	0.64[1]	0.71[1]		99.32	99.32

G is the GRACE particle, C is the $NiO/MgAl_2O_4$ particle
[1]from NiO-equilibrium, since the measured value of CO was lower than equilibrium and H_2 was not analysed.
[2]not analysed, assumed value based on CO and assuming water shift equilibrium.

4.3.3 Oxygen-carrier

Totally, the $NiO/MgAl_2O_4$ particle was fluidized 150 hours in hot conditions, of which 30 h were with combustion. No loss in reactivity was observed during the tests.

Before and after the test series the particles were weighed and there was a total loss in the mass balance of 13 g, or 4%, of the solids inventory. This corresponds to a loss of 0.027% per h. No measurable amounts of particles were found in the filters, so it is not clear how this mass was lost. Minor losses could be associated with the opening of the reactor system, leakages through pressure taps, and another possibility is deposits in the ducts leading to the filters. Reduction, i.e. reduced degree of oxidation, could be another cause for mass reduction, although the particles in the reactor system were run without fuel, i.e. oxidized before they were taken out. In total, the absence of fines in the filters and the low mass loss suggest that the particle have a high durability. It should be noted that the fluidization velocities are low, and not comparable with velocities expected in a full-scale fluidized-bed chemical-looping combustor.

The GRACE particles were run in this reactor under hot conditions for 18 hours, of which 8 h were with combustion. Before these tests, the same particles had been run in a 10 kW unit with more than 100 hours of combustion, (Lyngfelt and Thunman 2005).

5 CONCLUSIONS

Chemical-looping combustion has emerged as a promising technology for achieving CO_2 capture from combustion without large energy penalties. Thus, there has been a large amount of research conducted in the last years, mainly focusing on oxygen-carrier preparation and testing as well as system studies. However, there was also a need for better understanding of reactor system design and especially a smaller unit where particles can be tested in real operation was needed. This thesis has focused on the study of reactor systems and includes experimental results from two cold-flow models and one 300 W chemical-looping combustor. The first cold-flow model had a CFB-like design, whereas the second cold-flow model and the 300 W chemical-looping combustor had a two-chamber fluidized-bed system with a simplified system for circulation.

A CFB like reactor system was built in Perspex and in this solids circulation rate and gas leakage was investigated. The amount of bed material and gas velocity were varied to find suitable operation conditions. The main results from this study were:

- The relation between solids circulation and fluidizing velocity was determined for different solids inventories. The solids circulation rates studied were in a range sufficient for metal oxides like copper oxide, nickel oxide and manganese oxide. However, there was an uncertainty whether the flow is high enough for particles with lower oxygen transfer capacity like iron oxide, Fe_2O_3. It was not possible to achieve stable conditions during higher velocities because the inlet to the fuel reactor from the downcomer was limiting the circulation flow of particles.

- The gas leakage from the fuel reactor to the cyclone varied in the range 1-3.5%, with a typical value of 2%, which means that about 2% of the carbon dioxide will be lost to the atmosphere. In order to avoid this leakage it is possible to use steam for fluidizing, either in a separate pot-seal, or for the section right below the downcomer.

- The gas leakage from the pot-seal to the fuel reactor in the CFB design was significant. The produced carbon dioxide would be diluted with 2-15% air. This is most likely too high to be acceptable and motivates countermeasures, for instance fluidization with steam either below the downcomer or in the whole pot-seal.

It should be pointed out that gas leakage is not a major problem in this design of a CLC system since it can be avoided by using steam. However, it is important to estimate the leakage flows in order to assess the need for countermeasures.

Since there was a need to develop a small chemical-looping combustor for particle testing, a smaller two-compartment fluidized bed was investigated. It was first built and studied as a cold-flow model. After successful operation of the cold-flow model the corresponding 300 W chemical-looping combustor was built with some minor modifications compared to the cold-flow model design. From the tests in the cold-flow model and the 300 W chemical-looping combustor the following conclusions were made:

- Experiments with different flow model designs showed that it is possible to achieve sufficient circulation of particles for the oxygen transfer in a model running between 100 and 300 W. Since the laboratory system is to be placed in an oven, the energy balance of the system does not need to be met.

- The gas leakage between the reactors was low enough for a laboratory reactor, and in the hot design it was further reduced by changing the height and design of the slot, where particles are transferred from the fuel reactor to the air reactor. The possibility of fluidizing below the slot with inert gas was also introduced to reduce the gas leakage.

- Operation in the 300 W unit was successfully demonstrated using two fuels, natural gas and syngas consisting of 50% CO and 50% H_2, and two nickel-based oxygen-carriers.

- The design and operation of the 300 W chemical-looping combustor was satisfactory. The leakage was low enough to enable evaluation of the results, and the particle circulation was high enough to transport oxygen from the air to the fuel.

- The first particle tested in the 300 W unit and with natural gas as fuel, a nickel based particle, $NiO/MgAl_2O_4$, was found to be suitable as oxygen-carrier. It gave a high conversion of the natural gas. No methane was detected in the gas from the fuel reactor, and the fraction of CO varied between 0.5 and 3%. The combustion efficiency at 850˚C was 98.4%.

- No significant amount of fines was found after fluidization for 150 hours in hot conditions, of which 30 h were with combustion, which indicates that the $NiO/MgAl_2O_4$ particles had a high durability. It must be noted though, that the fluidization velocities are low, and not comparable with velocities expected in a full-scale fluidized-bed chemical-looping combustor. Furthermore, no loss in reactivity was observed during the tests.

- Syngas was also tested as fuel with the $NiO/MgAl_2O_4$ particle as oxygen-carrier. The tests were successful with high conversion of the fuel, often exceeding 99%. The fraction of CO leaving the reactor has a maximum value of 2%, and the H_2 has a maximum value of 1.8%. The concentrations of CO and H_2 were strongly correlated when different parameters were varied. The concentration of CO in the measurements is 17-37% higher than the concentration of H_2.

- With natural gas another NiO-based particle, called the GRACE particle, was also tested for comparison. Also this particle had a high conversion of the natural gas to carbon dioxide and water. However, there is an interesting difference between the

two particles when it comes to conversion of CH_4 compared to CO. With the $NiO/MgAl_2O_4$ particles there is no methane in the gas from the fuel reactor when natural gas is used as fuel, while the GRACE particle does not have full conversion of methane. On the other hand, the GRACE particle shows a higher conversion of CO close to thermodynamics equilibrium, which is also higher than the conversion attained for the $NiO/MgAl_2O_4$ particle. The total combustion efficiency for natural gas at 850˚C is 99% for the GRACE particle, and 98.4% for the $NiO/MgAl_2O_4$ particle.

NOTATION

A	cross-section area	[m^2]
d_p	particle diameter	[m]
D	dilution (eq 15)	[-]
f_i	fraction of species i (eq 17-21)	[-]
g	acceleration due to gravity	[m/s^2]
G_s	net solids flux	[kg/m^2s]
H_i	heating value	[J/kg]
L	bed geometry	[m]
L	leakage (eq 16)	[-]
m	actual mass of the oxygen-carrier in the reactor	[kg]
m_{ox}	mass of the oxygen-carrier when fully oxidized	[kg]
m_{red}	mass of the oxygen-carrier when fully reduced	[kg]
$\dot{m}_{air}$	mass flow of air (eq 6)	[kg/s]
$\dot{m}_{fuel}$	mass flow of fuel	[kg/s]
$\dot{m}_o$	stoichiometric mass flow of oxygen to be transferred between two reactors (eq 5)	[kg/s]
$\dot{m}_{sol}$	oxygen-carrier recirculation rate between the air and fuel reactor (eq 12)	[kg/s]
M	molar mass	[kg/kmol]
M_{circ}	circulation rate of particles	[kg/s]
p	pressure	[Pa]
P_{th}	thermal power	[W]
R_o	Oxygen ratio, i.e. the mass fraction of oxygen that can be used in the oxygen-carrier (eq 10)	[-]
S_r	stoichiometric ratio	[-]
T	temperature	[°C]
T_{FR}	temperature in the fuel reactor	[°C]
u	gas velocity	[m/s]
u_0	superficial velocity	[m/s]
u_{mf}	minimum fluidization velocity	[m/s]

U	volume flow	[m^3/s, L/min]
U_{AR}	volume flow in the air reactor	[L/min]
U_{DC}	volume flow in the downcomer	[L/min]
U_{FR}	volume flow in the fuel reactor	[L/min]
U_{SL}	volume flow in the slot	[L/min]
x_i	molar fraction of species i	[-]
X	conversion of oxygen-carrier, degree of oxidation	[-]
X_{ox}	conversion of the oxygen-carrier in the air reactor	[-]
X_{red}	conversion of the oxygen-carrier in the fuel reactor	[-]
ΔX	the difference in conversion	[-]
ϕ	particle coefficient	[-]
λ	air ratio	[-]
ρ	density	[kg/m^3]
ρ_f	density of the fluid	[kg/m^3]
ρ_s	density of the solids	[kg/m^3]
$\Delta\omega$	change of mass conversion of a cycle	[-]
ω	mass-conversion (eq 11)	[-]

REFERENCES

Abellon, R. D., Z. I. Kolar, W. den Hollander, J. J. M. de Goeij, J. C. Schouten and C. M. van den Bleek "A single radiotracer particle method for the determination of solids circulation rate in interconnected fluidized beds." *Powder Technology* (1997). **92**: 53-60.

Adánez, J., L. F. de Diego, F. García-Labiano, P. Gayán, A. Abad and J. M. Palacios "Selection of Oxygen Carriers for Chemical-Looping Combustion." *Energy and Fuels* (2004). **18**: 371-377.

Anheden, M., A.-S. Näsholm and G. Svedberg (1995). *Chemical-Looping Combustion -Efficient Conversion of Chemical Energy in Fuels into Work*. 30th Intersociety Energy Conversion Engineering Conference, IECEC, Orlando, USA. 75-81

Anheden, M. and G. Svedberg (1996). *Chemical-Looping Combustion in Combination with Integrated Coal Gasification*. 31th Intersociety Energy Conversion Engineering Conference, IECEC, Washington DC, USA, IEEE, Piscataway, NJ, USA. 2045-2050

Avidan, A. A. (1997). *Fluid Catalytic Cracking*. Circulating Fluidized Beds. J. R. Grace, A. A. Avidan and T. M. Knowlton, Chapman and Hall**:** 466-488.

Avidan, A. A. and R. Shinnar "Development of Catalytic Cracking Technology. A Lesson in Chemical Reactor Design." *Industrial and Engineering Chemistry Research* (1990). **29**: 931-942.

Azar, C. and H. Rodhe "Targets for Stabilization of Atmospheric CO_2." *Science* (1997). **276**: 1818-1819.

Bisio, G., L. Marletta and G. Rubatto (1998). *Two-Step Fuel Oxidation to Improve Efficiency in the Conversion of Chemical Exergy into Work*. Intersoc. Energy Conversion Eng. Conf.

Brandvoll, Ø. (2005) *Chemical Looping Combustion - Fuel Conversion with Inherent CO_2 Capture* PhD Thesis, Norwegian University of Science and Technology, Trondheim

Cho, P. (2005) *Development and Characterisation of Oxygen-Carrier Materials for Chemical-Looping Combustion* PhD Thesis, Chalmers University of Technology, Göteborg

Cho, P., T. Mattisson and A. Lyngfelt "Comparison of Iron-, Nickel-, Copper and Manganese-Based Oxygen Carriers for Chemical-Looping Combustion." *Fuel* (2004). **83**: 1215-1225.

Chong, Y. O., D. J. Nicklin and P. J. Tait "Solids Exchange Between Adjacent Fluid Beds Without Gas Mixing." *Powder Technology* (1986). **47**: 151-156.

Consonni, S. and F. Vigano "Decarbonized hydrogen and electricity from natural gas." *International Journal of Hydrogen Energy* (2005). **30**(7): 701.

Copeland, R. J., G. Alptekin, M. Cesario and Y. Gershanovich (2001). *A Novel CO_2 Separation System*. First National Conference on Carbon Sequestration, U.S. Department of Energy, National Energy Technology Laboratory, Pittsburgh, PA, USA.

Davis, M. (1986). *Climatic Change and the Survival of Forest Species*. The Earth in Transition - Patterns and Processes of Biotic Impoverishment. G. M. Woodwell, Cambridge University Press**:** 99-110.

Fang, M., C. Yu, Z. Shi, Q. Wang, Z. Lou and K. Cen "Experimental research on solid circulation in a twin fluidized bed system." *Chemical Engineering Journal* (2003). **94**: 171-178.

Fox, D., Y. Molodtsof and J. F. Large "Control Mechanisms of Fluidized Solids Circulation Between Adjacent Vessels." *AIChE Journal* (1989). **35**(12): 1933-1941.

Glicksman, L. R., M. R. Hyre and K. Woloshun "Simplified scaling relationships for fluidized beds." *Powder Technology* (1993). **77**: 177-199.

Harvey, D. L. D. (2000). *Global Warming - The Hard Science*. Singapore, Pearson Education Limited.

Harvey, S. P. (1994) *Reversibility of Combustion Processes* PhD Thesis, Dartmouth College, Hanover

Hatanaka, T., S. Matsuda and H. Hatano (1997). *A Mew-Concept Gas-Solid Combustion System "MERIT" for High Combustion Efficiency and Low Emission*. Intersociety Energy Conversion Engineering Conference, Honolulu, Hawaii. 944-948

He, Y., V. Rudolph, D. J. Nicklin and Y. O. Chong "Circulating Fluidized Oil Shale Retort." *Fuel* (1993). **72**(6): 879-883.

IPCC (1998). *The Regional Impacts of Climate Change - An Assessment of Vulnerability*, Cambridge University Press.

IPCC (2001). *Climate Change 2001 - The Scientific Basis*, Cambridge University Press.

Ishida, M. and H. Jin "A new Advanced Power-Generation System using Chemical-Looping Combustion." *Energy* (1994). **19**(4): 415-422.

Ishida, M., M. Yamamoto and T. Ohba "Experimental results of chemical-looping combustion with $NiO/NiAl_2O_4$ particle circulation at 1200 °C." *Energy Conversion and Management* (2002). **43**: 1469-1478.

Ishida, M., D. Zheng and T. Akehata "Evaluation of a Chemical-Looping-Combustion Power-Generation System by Graphic Exergy Analysis." *Energy* (1987). **12**(2): 147-154.

Jin, H., T. Okamoto and M. Ishida "Development of a Novel Chemical-Looping Combustion: Synthesis of a Solid Looping Material of $NiO/NiAl_2O_4$." *Industrial and Engineering Chemistry Research* (1999). **38**: 126-132.

Johansson, M., T. Mattisson and A. Lyngfelt (2005). *Comparison of Oxygen Carriers for Chemical-Looping Combustion*. International Symposium: Moving towards zero-emission plants, Leptokarya Piera, Greece, CERTH/ISTFA.

Kehlenbeck, R., J. G. Yates, D. Cheesman, R. di Felice, H. Hofbauer and R. Rauch "Experimentelle Untersuchungen in einer Zirkulierenden Wirbelschicht zum Vergasen von Biomasse." *Energie aus Biomasse* (2001). **73**: 1215-1218.

Kronberger, B., A. Lyngfelt, G. Löffler and H. Hofbauer "Design and Fluid Dynamic Analysis of a Bench-Scale Combustion System with CO_2 Separation - Chemical-Looping Combustion." *Industrial and Engineering Chemistry Research* (2005). **44**: 546-556.

Kunii, D. and O. Levenspiel (1991). *Fluidization Engineering*. Stoneham, Reed Publishing Inc.

Kuramoto, M., D. Kunii and T. Furusawa "Flow of Dense Fluidized articles through an Opening in a Circulation System." *Powder Technology* (1986). **47**: 141-149.

Lyngfelt, A., B. Kronberger, J. Adanez, J. X. Morin and P. Hurst (2004). *The Grace Project. Development of Oxygen Carrier Particles for Chemical-Looping Combustion. Design and Operation of a 10 kW Chemical-Looping Combustor.* 7th International Conference on Greenhouse Gas Control Technologies, Vancouver, Canada.

Lyngfelt, A., B. Leckner and T. Mattisson "A fluidized-bed combustor process with inherent CO_2 separation; application of chemical-looping combustion." *Chemical Engineering Science* (2001). **56**: 3101-3113.

Lyngfelt, A. and H. Thunman (2005). *Construction and 100 h of Operational Experience of a 10-kW Chemical Looping Combustor*. Carbon Dioxide Capture for Storage in Deep Geologic Formations - Results from the CO2 Capture Project. D. Thomas, Elsevier Science. **1 - Capture and Separation of Carbon Dioxide From Combustion Sources:** 625-646.

Mattisson, T., M. Johansson and A. Lyngfelt "Multi-Cycle Reduction and Oxidation of Different Types of Iron Oxide Particles - Application to Chemical-Looping Combustion." *Energy and Fuels* (2004). **18**: 628-637.

Mattisson, T. and A. Lyngfelt (2001). *Capture of CO_2 Using Chemical-Looping Combustion*. First Biennial Meeting of Scandinavian-Nordic Section of the Combustion Institute, Göteborg, Sweden. 163-168

Mattisson, T., A. Lyngfelt and P. Cho "The Use of Iron Oxide as an Oxygen Carrier in Chemical-Looping Combustion of Methane with Inherent Separation of CO_2." *Fuel* (2001). **80**: 1953-1962.

Morin, J. X. and C. Béal (2005). *Chemical Looping Combustion of Refinery Fuel Gas with CO_2 Capture*. Carbon Dioxide Capture for Storage in Deep Geologic Formations - Results from the CO_2 Capture Project. D. Thomas, Elsevier Science. **1 - Capture and Separation of Carbon Dioxide From Combustion Sources:** 647-654.

Naqvi, R., O. Bolland, O. Brandvoll and K. Helle (2004). *Chemical looping combustion-analysis of natural gas fired power cycles with inherent CO_2 capture*, Vienna, Austria, American Society of Mechanical Engineers, New York, NY 10016-5990, United States. 301

NE (2005). *Nationalencyclopedin*, www.ne.se.

Pfeifer, C., R. Rauch and H. Hofbauer "In-Bed Catalytid Tar Reduction in a Dual Fluidized Bed Biomass Steam Gasifier." *Industrial and Engineering Chemistry Research* (2004). **43**: 1634-1640.

Richter, H. J. and K. F. Knoche "Reversibility of Combustion Processes." *ACS Symposium Series* (1983). **235**: 71-85.

Ryu, H. J., G.-T. Jin and C.-K. Yi (2004). *Demonstration of Inherent CO_2 Separation and no NO_x Emission in a 50 kW Chemical-Looping Combustor: Continuous Reduction and Oxidation Experiment*. 7th International Conference on Greenhouse Gas Control Technologies, Vancouver, Canada. Poster

Snieders, F. F., A. C. Hoffmann, D. Cheesman, J. G. Yates, M. Stein and J. P. K. Seville "The dynamics of large particles in a four-compartment interconnected fluidized bed." *Powder Technology* (1999). **101**: 229-239.

Snip, O. C., M. Woods, R. Korbee, J. C. Schouten and C. M. van den Bleek "Regenerative removal of SO_2 and NO_x for a 150 MWe power plant in an interconnected fluidized bed facility." *Chemical Engineering Science* (1996). **51**(10): 2021-2029.

Song, K., Y. Seo, H. Yoon and S.-H. Cho "Characteristics of the NiO/Hexaaluminate for Chemical-Looping Combustion." *Korean Journal of Chemical Engineering* (2003). **20**(3): 471-475.

Strömberg, L. (2001). *Combustion in a CO_2/O_2 Mixture for a CO_2 Emission Free Process*. Second Nordic Minisymposium on Carbon Dioxide Capture and Storage, Gothenburg, Sweden. 58-63

Sundkvist, S.-G., T. Griffin and N. P. Thorshaug (2001). *AZEP - Development of an Integrated Air Separation Membrane - Gas Turbine*. Second Nordic Minisymposium on Carbon Dioxide Capture and Storage, Göteborg, Sweden. 52-57

Walther, G.-R., E. Post, P. Convey, A. Menzel, C. Parmesan, T. J. C. Beebee, J.-M. Fromentin, O. Hoegh-Guldberg and F. Bairlein "Ecological Responses to Recent Climate Change." *Nature* (2002). **416**: 389-395.

Villa, R., C. Cristiani, G. Groppi, L. Lietti, P. Forsatti, U. Cornaro and S. Rossini "Ni Based Mixed Oxide Materials for CH_4 Oxidation under Redox Cycle Conditions." *Journal of Molecular Catalysis A: Chemical* (2003). **204-205**: 637-646.

Wolf, J. (2004) *CO2 Mitigation in Advanced Power Cycles -Chemical Looping Combustion and Steam-Based Gasification* Doctoral Thesis, KTH - Royal Institute of Technology, Stockholm

Yu, J., A. Corripio, D. Harrison and R. J. Copeland "Analysis of the Sorbent Energy Transfer System (SETS) for Power Generation and CO_2 Capture." *Advanced Environmental Research* (2003). **7**: 335-345.